Review Article

Nano Research
2022, 15(11): 9850–9865

ISSN 1998-0124 CN 11-5974/O4
https://doi.org/10.1007/s12274-022-4272-z

Preparation and application of graphene-based wearable sensors

Shan Xia[1], Ming Wang[1], and Guanghui Gao[1,2] (✉)

[1] *Polymeric and Soft Materials Laboratory, School of Chemical Engineering and Advanced Institute of Materials Science, Changchun University of Technology, Changchun 130012, China*
[2] *Beijing Graphene Institute (BGI), Beijing 100871, China*

Received: 13 December 2021 / **Revised:** 26 January 2022 / **Accepted:** 23 February 2022

ABSTRACT

With the development of digital healthcare technology, the demand for non-invasive monitoring of human health is rapidly increasing. In recent years, the research and application of timely, economical, and easy-to-operate wearable sensing devices have attracted much attention. Among recent studies, graphene has been widely used to improve the sensing performance of wearable sensors due to its advantages in mechanical, electrical, and thermal properties. This review mainly focuses on summarizing graphene and its derivative-based wearable sensors and their latest developments in personal health monitoring. We will first introduce the novel structure and sensing mechanism of different types of graphene sensors. Then, we summarize the latest applications of the graphene wearable sensors in human health monitoring, including human activity, heart rate, pulse, electrophysiological signal, and electronic skin. Finally, the future challenges and prospects of graphene wearable devices will be discussed.

KEYWORDS

graphene, sensor, health monitoring, physiological signal, electronic skin

1 Introduction

Wearable sensors are portable devices that can be worn or installed on the human body to sense, transmit, and process information [1–5]. They have been widely used in consumer sports, fitness, and health fields. In recent years, patients with chronic diseases such as cardiovascular disease, hypertension, and diabetes have been increasing, occupying a large number of medical resources [6–8]. Real-time tracking of key health indicators such as heart rate, blood pressure, pulse, respiratory rate, and blood sugar level is particularly important for early diagnosis of chronic diseases and timely detection of life-threatening conditions such as seizures and cardiac arrest [9–14]. With the rapid growth in demand for continuous health monitoring and seamless human–computer interaction, wearable devices are rapidly expanding into the healthcare field, and the market is expected to reach 32 billion U.S. dollars by 2024 [15]. The application of wearable devices in the medical field makes it possible to provide personalized medical services, reduce hospitalization rates, and prevent avoidable deaths, greatly reducing the pressure on doctors and the healthcare system.

To meet daily activities and prevent pathogens from invading, human skin presents a rough and dynamic curved surface [16–18]. However, there is a serious mechanical mismatch between commercial rigid sensors and human skin, making it difficult to form a tight interface between them, resulting in increased interface impedance and greatly reduced detection quality of human body signals [19–22]. In addition, the human body is a "precision machine" full of sensors, producing different forms of physiological signals at all times [23–25]. The physiological signals produced by the human body mainly include mechanical signals, electrocardiograms (ECG) [26, 27], electromyograms (EMG) [28], electroencephalograms (EEG) [29], and other electronic signals generated by human movements, as well as electrochemical signals such as ions in body fluids and glucose [30, 31]. To achieve accurate, real-time, and continuous monitoring of these signals, the sensor must have high specificity and sensitivity. In addition to good signal detection functions, factors such as miniaturization, comfort, low cost, and long-term use should also be considered to meet the different needs of daily life [32–34].

With its excellent electrical conductivity, flexibility, thermal conductivity, carrier mobility, and mechanical strength, graphene has attracted widespread attention in the development of wearable devices for health monitoring and electrophysiological signal detection [35–38]. Graphene sensors used in wearable electronic products show outstanding potential for future telemedicine. Graphene is a two-dimensional (2D) atomic sheet of sp^2-carbon, which is a promising 2D material in many applications [39–42]. In addition, graphene can also be processed into various shapes of one-dimensional (1D) fibers, 2D films, and three-dimensional (3D) structures for precise integration into various wearable devices [43]. The reported graphene sensor can not only acquire mechanical signals such as human motion, respiration, and pulse sound, but also accurately detect electrophysiological signals signals [44–50]. So far, graphene, original graphene, graphene oxide (GO), and reduced GO (rGO), have been widely studied and highly recognized in the field of flexible sensors [51–58].

Address correspondence to ghgao@ccut.edu.cn

In this review, we summarize the latest developments in graphene wearable sensors for health monitoring, human–machine interfaces, and electronic skin (E-skin) (Fig. 1). First, we briefly overview the preparation methods of graphene and its derivatives, as well as their advantages and limitations in wearable sensing devices. Next, the newest innovations in the structure, sensing mechanism, and manufacturing technology of graphene sensing devices are discussed. Subsequently, we focused on the recent applications of graphene wearable sensors in non-invasive human health monitoring, human–machine interfaces, and artificial prostheses. Finally, potential challenges and prospects of graphene wearable sensors will be discussed.

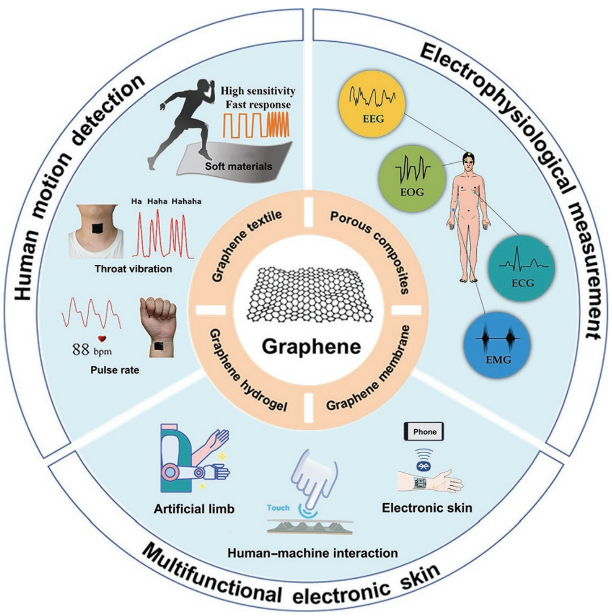

Figure 1 Brief of graphene-based wearable sensor systems for personalized healthcare management. Reproduced with permission from Ref. [53], © The Royal Society of Chemistry 2019.

2 Performances of graphene in wearable sensors

According to different structures and sensing materials, wearable sensors can be divided into piezoresistive, piezoelectric, capacitive, and triboelectric sensing mechanisms [59, 60]. Among them, piezoresistive sensors that measure resistance changes are often used in the design of pressure, tactile, and strain sensors due to their simple design and convenient data acquisition [19, 60]. Wearable piezoresistive sensors should have the characteristics of high sensitivity, wide detection range, fast responsibility, and durability to achieve accurate dynamic human activity monitoring [32, 33]. The performance diversity of graphene is beneficial to realize multifunctional piezoresistive sensors. First, the high conductivity can improve the sensitivity of graphene sensors, enabling efficient signal transmission and high signal-to-noise ratio [61, 62]. In addition, the ultra-thin thickness and ultra-high mechanical flexibility of graphene help to achieve conformal contact with human skin, tissues, and organs, which is crucial for reducing motion artifacts and improving signal quality [63]. Moreover, the excellent optical transparency of graphene is beneficial to achieve clear images without visual interference, which has important applications in the fields of electronic skin and soft robotics [64]. In addition, due to its ultra-high specific surface area, graphene can effectively immobilize receptors such as gases, chemicals, and diverse biological molecules, making it suitable carriers for chemical sensors and biosensors [65, 66].

3 Graphene and its derivatives

3.1 Synthesis and properties of graphene

The synthesis of high-quality graphene is essential for the manufacture of graphene-based wearable sensors that can be used in practical applications [67, 68]. Since the first preparation by mechanical exfoliation of graphite in 2004, various methods have been developed to synthesize graphene materials with different structures [69]. So far, the manufacturing methods of graphene are mainly top-down (TD) and bottom-up (BU) approaches [70]. Among them, the TD method is scalable and low-cost, including micromechanical exfoliation [71], solution exfoliation [72], and unzipping of carbon nanotubes (CNTs) [73]. However, the manufacturing process usually involves breaking large pieces of carbon into thinner and smaller graphene sheets, causing unavoidable defects [71]. The BU method is to assemble large-scale graphene layers or structures from carbon atoms, including chemical vapor deposition (CVD) growth [74, 75], epitaxial growth [76, 77], and all-organic synthesis [78]. Compared with the TD method, the BU technology can produce graphene with fewer defects and high quality, but it is expensive and difficult to produce on a large scale, hindering its wide application.

Graphene is a honeycomb lattice structure formed by densely packed sp^2-hybridized carbon atoms. The unique lattice structure and atomic thickness endow it with excellent mechanical, electronic, optical, and physicochemical properties, which have received extensive attention in the electrochemical field [61, 63, 79]. Due to the perfect arrangement of atoms, graphene exhibits excellent mechanical properties and is even harder than the well-known natural diamond. Columbia University physicist Li conducted a comprehensive study on the mechanical properties of graphene. The report proved that the tensile strength of monolayer graphene reached 130 GPa, Young's modulus was as high as 1 TPa, and the breaking strength was 200 times that of steel [80]. Unlike graphite, graphene has a unique zero bandgap and semi-metallic properties. More importantly, the unique electronic properties of these zero energy gap points make graphene highly conductive. The carrier mobility of single-layer graphene reaches 200,000 $cm^2/(V \cdot s)$, and the resistivity of graphene is about 10^{-6} $\Omega \cdot cm$, which is smaller than known silver with the smallest resistivity [81]. Due to its anisotropic structure, graphene has a very high thermal conductivity. The thermal conductivity of pure defect-free single-layer graphene is as high as 5,300 $W/(m \cdot K)$, which is much higher than that of single-walled carbon nanotubes [82, 83]. Graphene also has special optical properties, and the transparency of single-layer graphene is as high as 97.7%, showing great potential in optical electronic devices and foldable devices [64]. Excellent mechanical properties, high thermal conductivity, and high electron mobility make graphene an ideal candidate for ultra-sensitive detection of various physiological signals and daily activities of the human body.

3.2 GO and rGO

GO and rGO are popular and attractive as alternatives to graphene due to the simple preparation methods and easy scale-up production [84–89]. GO has a large number of hydrophilic oxygen-containing functional groups on the surface and edges, such as carboxyl (–COOH), alkoxy (C–O–C), hydroxyl (–OH), carbonyl (C=O), and other functional groups, which greatly improve the solubility and dispersion of graphene in both organic and aqueous solvents [90–92]. This is conducive to the composite with metals, metal oxides, polymers, and other materials, greatly broadening the application fields of graphene [93–95]. However, during the oxidation process, the addition of oxygen lattice causes distortion of the carbon lattice, destroying the highly conjugated structure of graphene. To obtain the structure and characteristics close to the original graphene, the reduction method is often used to remove the oxygen lattice of the graphene oxide [96–100]. Although the obtained rGO contains residual oxygen and other heteroatoms and structural defects, it still retains properties similar to graphene. In addition, the morphology and chemical properties of rGO can be adjusted according to different preparation methods. The rGO is suitable for related applications that replaces graphene, such as composite materials, conductive inks, and sensors [101–103].

4 Graphene wearable devices

In the last decade, wearable flexible electronic devices have developed rapidly, showing potential applications in human motion monitoring, medical rehabilitation, and software robots [104–107]. Although wearable sensors based on different materials have been developed for a long time, graphene-based sensors have shown great potential in the development and application of wearable electronic devices due to the excellent mechanical and electrical properties of graphene itself. Moreover, graphene and its derivatives are often used in the manufacture of wearable sensors due to their excellent piezoresistive properties and easy processing.

Wearable sensors usually consist of three parts: (1) flexible substrates to support other materials and accommodate the irregular surface of the target, (2) sensing elements to convert other input signals into visual electrical signals, and (3) electrodes for electric signal output [108, 109]. In recent years, graphene composite materials with different structures have been used to assemble flexible sensors for sensing applications. Among them, flexible graphene films [110], graphene textiles [111, 112], porous graphene composites [113–117], and graphene composite hydrogels [118–121] are the common forms of graphene piezoresistive sensor, which can not only monitor physiological parameters such as heart rate, body surface temperature, blood oxygen level, and exercise volume, but also important physiological indicators related to inflammation and even insulin.

4.1 Graphene film sensors

The wearable platform used for health monitoring should be tightly attached to the skin for continuous noise-free signal detection. Therefore, the thinness and flexibility of wearable sensors are essential for forming conformal contact with the human body to improve sensing sensitivity [122–126]. In the sensor system, the flexible substrate used to support conductive material and sensing element is the key to determining the flexibility and stretchability of wearable sensors. The most commonly used substrates with excellent elasticity and flexibility are polydimethylsiloxane (PDMS) [127–129], ecoflex [130, 131], polyethylene terephthalate (PET) [132–134], and polyimide (PI) [135–137].

Chen et al. [128] reported laser-induced graphene (LIG) electronic skin by one-step CO_2 laser scribing of a polyamide film, and systematically studied the effects of laser parameters and LIG patterns on the mechanical and sensing properties of the

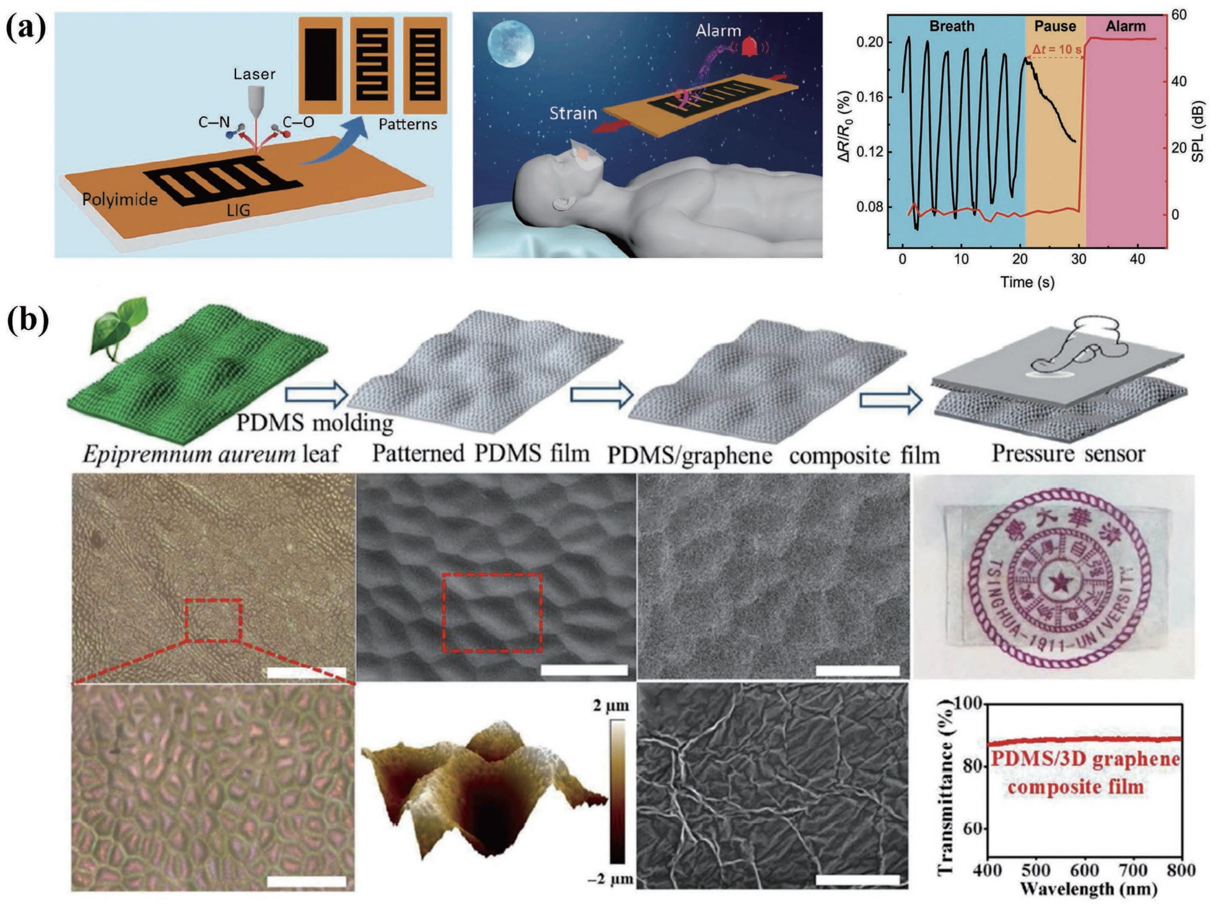

Figure 2 Synthesis and application of graphene film sensors. (a) The preparation process of LIG electronic skin and its application in human motion detection. Reproduced with permission from Ref. [128], © WILEY-VCH Verlag GmbH & Co. KGaA, Weinheim 2019. (b) Preparation, structure, and performance characterization of CVD-grown 3D graphene film sensor. Reproduced with permission from Ref. [129], © Tsinghua University Press and Springer-Verlag Berlin Heidelberg 2017.

electronic skin (Fig. 2(a)). Various patterns could be designed by controlling the scanning path of the laser, such as square, zigzag, and shutter. By optimizing the laser parameters and LIG patterns, the LIG electronic skin achieved an ultra-high sensitivity of up to 316.3. Based on the superior performances, the unique patterned E-skin could be used not only for physiological signal detection but also as voice recognition and sound alarm device.

Xia et al. [129] prepared a flexible membrane pressure sensor based on CVD-grown 3D graphene film (Fig. 2(b)). The graphene film was obtained by electrochemical deposition growth as a sensing element to imitate the skin texture of the fingertip, and PDMS with a hierarchical structure was used as an elastic support material to obtain an ultra-thin, sensitive, and skin-compliant membrane sensor. The unique bionic layered structure endowed the graphene sensor with high sensing performance, such as high sensitivity (110 kPa^{-1} for 0–0.2 kPa), fast response time (< 30 ms), and low detection limit (0.2 Pa).

4.2 Graphene textile sensors

Wearable textile devices that can be integrated into everyday clothing have practical and easy-to-sensing characteristics [138–140]. Natural textile materials have a unique crisscross woven structure, which can be used to connect conductive nanomaterials to form a continuous conductive path. By combining textile fiber materials with various conductive materials, the unique structure greatly improves the performance of conductive textiles, making it an ideal substrate for tactile sensors. Compared with traditional wearable devices, electronic textiles have the characteristics of breathability, portability, abrasion resistance, and high shape adaptability [141–146]. At present, there are many methods for fabricating graphene textile sensors, including thermal-transfer process, electrospray deposition (ESD) technology weaving, surface-pasting, screen printing, chemical vapor deposition and so on.

Wei et al. [147] obtained the reduced graphene oxide pattern through a laser scribing process, and then thermally transferred the customized pattern to the textile to obtain a multifunctional intelligent graphene textile device (Fig. 3(a)). The method was simple to prepare, low in cost, and time-saving. The graphene textiles exhibited high linearity under strain and pressure testing, with determination coefficients exceeding 99.3% and 98.2%, respectively, which was expected to bring broader practical prospects for *in-situ* health monitoring.

Han et al. [148] used commercial polyester fabric as a substrate, deposited GO on its surface by ESD technology, and then annealed and rGO-coated fabric by thermal reduction (Fig. 3(b)). The ESD technology was simple and easy to operate, which greatly improved the interface combination of graphene and textiles, and gave full play to the excellent structure of textiles and the sensing properties of graphene. Based on the unique interweaving structure, rGO textiles exhibited good sensing characteristics for strain and pressure in different directions, which could monitor large transverse deformation of the human motion as well as longitudinal breathing, pulse, and other pressure signals.

Currently, most graphene electronic textiles are manufactured by combining discrete graphene with textile materials. However, during the frequent stretching process, the unmatched mechanical properties of the two parts cause the interface to separate. Chen et al. [149] proposed a method of using 3D printing technology to develop a smart graphene textile with a core-sheath structure (Fig. 3(c)). Graphene was used as the conductive core layer, and poly(tetrafluoroethylene) (PTFE) particles and PDMS were used

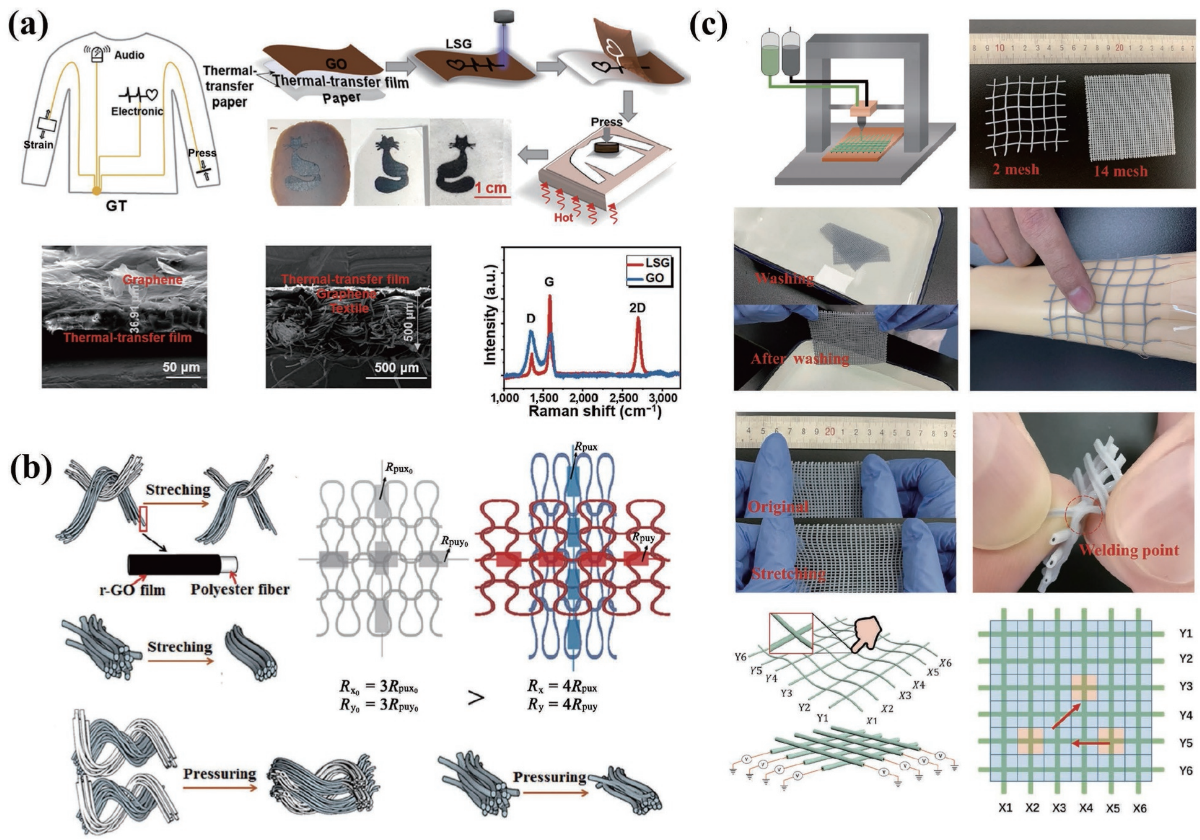

Figure 3 (a) Schematic fabrication process and characterization of the graphene textiles through a laser scribing and pattern thermal transfer process. Reproduced with permission from Ref. [147], © American Chemical Society 2021. (b) Schematic illustration of the structure and mechanism of the rGO textile deposited by ESD technology. Reproduced with permission from Ref. [148], © Tsinghua University Press and Springer-Verlag GmbH Germany, part of Springer Nature 2021. (c) The formation process for stretchable smart textile fabricated by 3D printing technique and its wearable sensing performance. Reproduced with permission from Ref. [149], © Elsevier Ltd. 2021.

as the sheath layer. By adjusting the rheological properties of the prepolymer, continuous stretchable graphene fibers were obtained through 3D printing technology. This method eliminated the complicated weaving process of traditional textiles and could customize the production scale. The produced smart fiber textile exhibited excellent stretchability with elastic modulus of 0.12 MPa and tensile strength of 0.22 MPa, structural stability, abrasion resistance, and washability, and had great potential in wearable tactile sensing.

4.3 Porous graphene composites (aerogel, foam, and sponge) sensors

Constructing the surface microstructure is an effective strategy to improve the sensing performance of the sensor. However, the delicate surface microstructure often exhibits a limited working range and sensitivity decay under high temperature or high pressure. Materials with porous structures (sponge [150–154], foam [155–159], aerogel [160–166], etc.) have received widespread attention in piezoresistive sensors. The porous structure with high compressibility and elasticity can withstand a wide range of deformation and exhibits obvious resistance changes even under slight deformation.

Aerogel is attractive in wearable sensors due to its compressibility, elasticity, and ultra-light advantages. To achieve excellent performance, Long et al. [165] used calcined GO, cellulose nanofiber (CNFs), glucose, and kaolin to construct a composite carbon aerogel (C-NGGK) with a low-density and continuous wave-shape structure (Fig. 4(a)). Carbon aerogels exhibited enhanced mechanical properties, super elasticity, and high compressibility, which could maintain the initial height and 77.2% stress after 2,000 cycles at 50% strain. The C-aerogel 5 can almost maintain the initial height and 77.2% of stress after 2,000 cycles under a strain of 50%. In addition, benefiting from its unique structure, the conductivity of C-NGGK was highly sensitive to compressive strain.

To meet the application requirements of wearable devices, elasticity and fatigue resistance have always been challenges for all-carbon aerogels. As shown in Fig. 4(b), Huang et al. [166] fabricated a full-carbon aerogel with a multi-arch structure by a two-stage solvothermal method. The author first used the secondary deep reduction method to improve the volume densification of the rGO hydrogel. Subsequently, a multi-arch structure of reduced graphene oxide aerogel was obtained through continuous directional freezing treatment. The two-step process of reducing GO and unidirectional ice growth successfully prepared all-carbon aerogels with excellent compressibility and elasticity. Based on its excellent mechanical strength and electrical conductivity, the aerogel had a stable stress response (10,000 cycles) and adjustable linear sensitivity.

Lu et al. [167] proposed an environmentally friendly and economical method for preparing lightweight conductive thermoplastic polyurethane (TPU) foams, including freeze-drying, dip-coating, and chemical reduction processes (Fig. 4(c)). The TPU foam obtained by freeze-drying was immersed in GO solution, and the rGO/TPU was obtained by reducing treatment with VC solution under vacuum. The immersion and reduction treatment makes the rGO conductive filler uniformly coated on the TPU frame to form a uniform conductive path. By controlling the immersion time, the conductivity of the rGO/TPU foam could be adjusted to achieve high-pressure sensitivity. Finally, rGO/TPU foam had high compressibility (up to 90%), high sensitivity (0.0152 kPa^{-1}), wide pressure detection range, and excellent stability.

Guan et al. [168] used sustainable natural wood as the skeleton and coated rGO nanosheets as a conductive material to prepare a high-performance rGO-coated wood sponge (rGO@WS) (Fig. 4(d)). The unique layered structure had high elasticity and good fatigue resistance. The introduction of rGO provided rGO@WS with high conductivity and sensitivity in a wide range of deformation. The piezoresistive sensor of rGO@WS exhibited

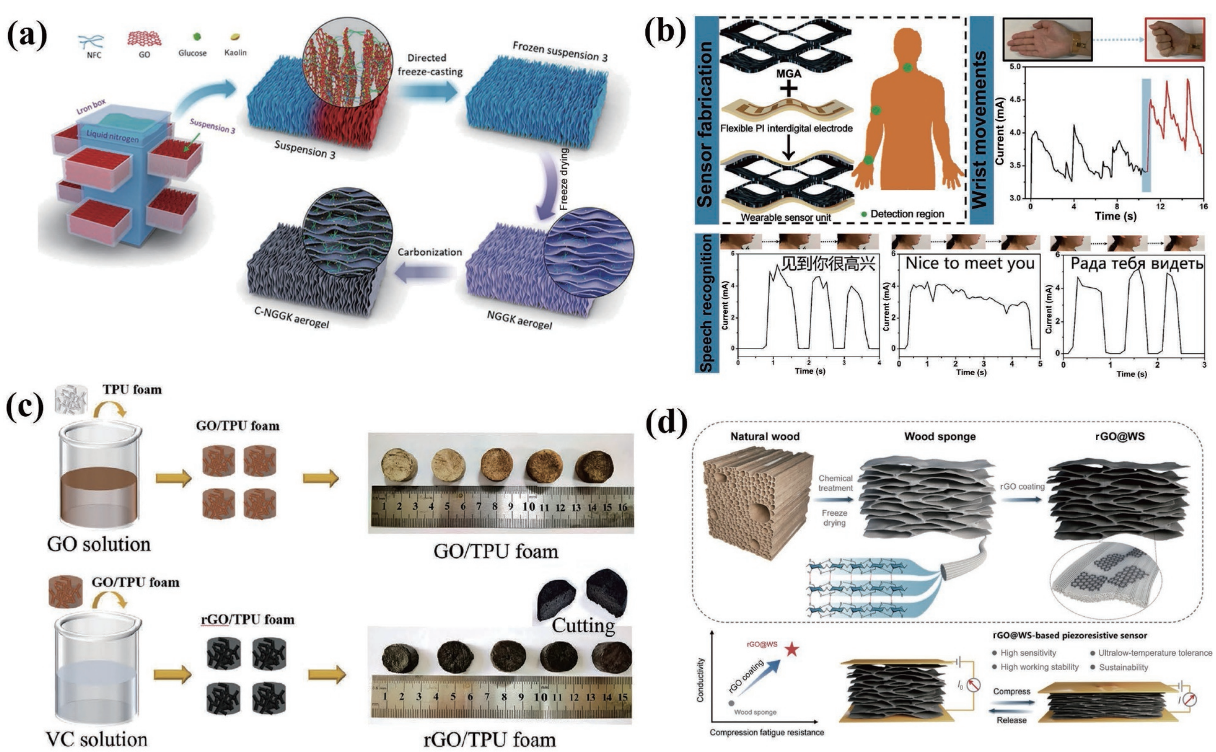

Figure 4 (a) Schematic illustration of the formation mechanism of the C-NGGK aerogel. Reproduced with permission from Ref. [165], © Elsevier Ltd. 2019. (b) Schematic illustration of the all-carbon aerogels for wearable sensors and detection of human motion. Reproduced with permission from Ref. [166], © American Chemical Society 2020. (c) The fabrication process of the rGO/TPU foam for the wearable sensor. Reproduced with permission from Ref. [167], © Wiley-VCH GmbH 2021. (d) Schematic illustration of the high-performance rGO@WS. Reproduced with permission from Ref. [168], © American Chemical Society 2021.

high working stability (over 10,000 cycles), high sensitivity (0.32 kPa^{-1}), low detection limit (30 Pa), and low temperature (−196 °C) sensing tolerance, which could be used to monitor human movement. In addition, the sensor array based on rGO@WS exhibited excellent spatially resolved pressure mapping in a large area, showing promising potential in human–computer interaction and electronic skin.

4.4 Graphene hydrogel sensors

Hydrogel is a soft material with a structure similar to that of natural tissues, showing excellent biocompatibility, softness, and flexibility [169–171]. Conductive hydrogel, which combines the electrochemical properties of conductive polymers and the softness of hydrogels, has been widely welcomed in the field of health monitoring in the past ten years, especially as wearable sensors and bioelectrodes that directly contact the human skin. However, most conductive hydrogels exhibit poor mechanical properties, making it difficult to adapt to long-term and repeated external forces and deformations, which hinders their wearable sensing applications [172–175]. Therefore, overcoming the inherent mechanical weakness is always a problem and challenge for conductive hydrogels. Based on the reinforcement mechanism of nanocomposites, high-strength graphene shows obvious advantages in enhancing the mechanical properties of hydrogels. However, graphene tends to aggregate in a hydrophilic polymer network, resulting in significant degradation in the electrical properties of the graphene incorporated into the hydrogel [176–178].

Compared with graphene, GO has better water solubility and obvious advantages in enhancing the performances of hydrogels. As shown in Fig. 5(a), He et al. [179] used silk fibroin and GO to synergistically enhance the mechanical strength of polypropylene ammonium hydrogel. However, due to the weaker conductivity of GO, a conductive polymer (poly(3,4-ethylenedioxythiophene):polystyrenesulfonic acid (PEDOT:PSS)) was further introduced to improve the conductivity of the polyacrylamide/silk fibroin/GO/PEDOT:PSS (PSGP) hydrogel.

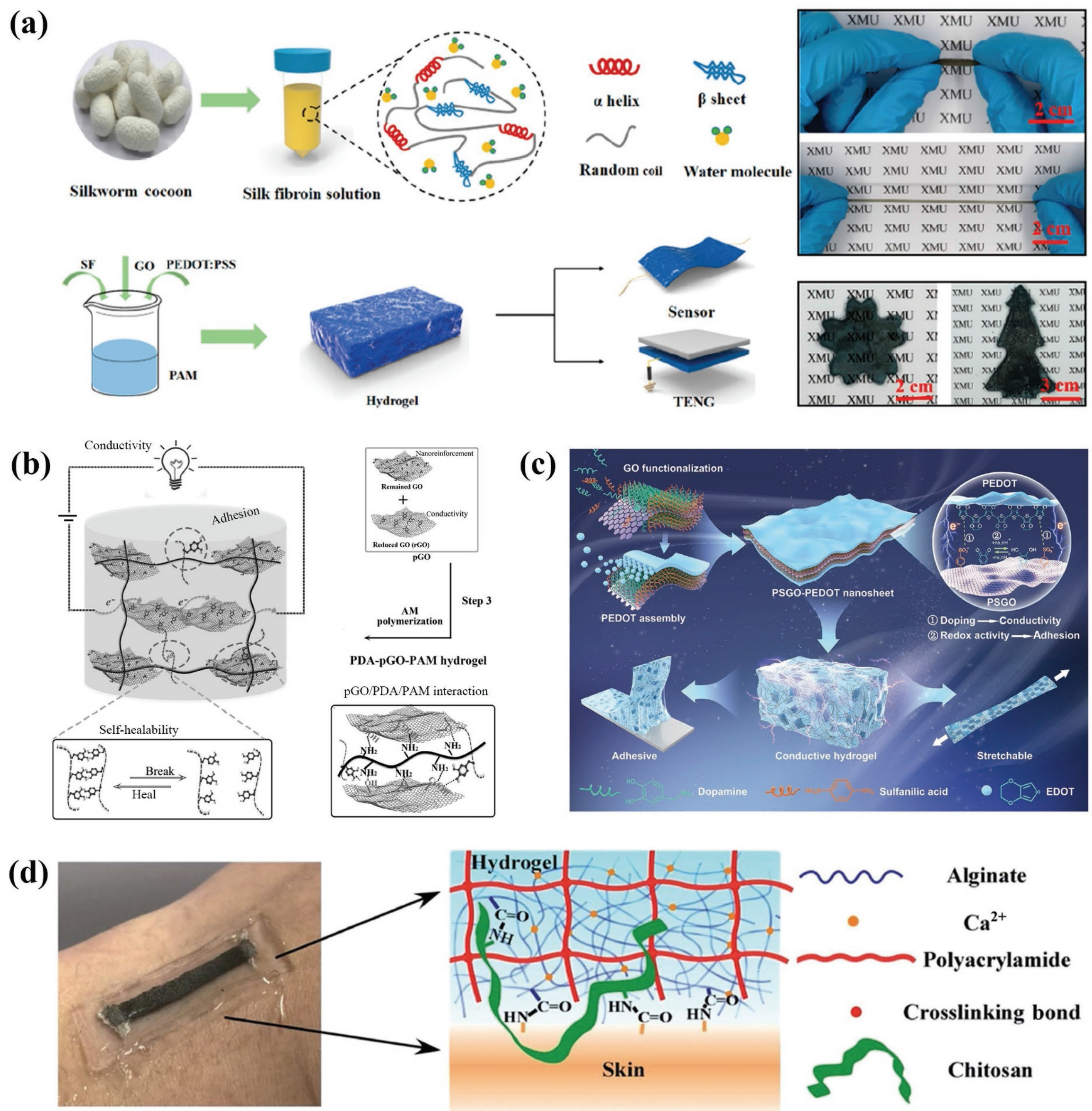

Figure 5 (a) Schematic illustration of the fabrication procedures and structures of the PSGP hydrogel for a high-performance wearable sensor. Reproduced with permission from Ref. [179], © American Chemical Society 2020. (b) Schematic fabrication process of PDA-rGO hydrogel. Reproduced with permission from Ref. [180], © Wiley-VCH Verlag GmbH & Co. KGaA, Weinheim 2016. (c) The preparation process and sensing principle of hydrogel incorporated PSGD nanosheets. Reproduced with permission from Ref. [181], © WILEY-VCH Verlag GmbH & Co. KGaA, Weinheim 2019. (d) Schematic diagram of the hydrogel-based sensor by integrating graphene foam and the PAM/CA hydrogel. Reproduced with permission from Ref. [182], © The Royal Society of Chemistry 2019.

The obtained hydrogel had both stretchability and conductivity, and could be assembled into a strain sensor and a triboelectric nanogenerator for monitoring the physiological signals.

To solve the above problems, Han et al. [180] successfully prepared rGO hydrogels using polydopamine (PDA) as a modifier and reducing agent, inspired by mussel chemistry (Fig. 5(b)). Polydopamine is rich in catechol groups and shows excellent adhesion to the surface of a variety of materials. In this system, PDA could be used as a reducing agent and dispersant for GO. On the one hand, it helped to partially reduce GO to rGO, and at the same time, it could be entangled with rGO to form a conductive path. The obtained PDA-rGO hydrogel exhibited a good conductivity (0.18 S/cm), which could be used to detect applied signals and regulate cell activities. Gan et al. [181] were also inspired by mussels to obtain nanosheets with water solubility, conductivity, and redox activity by self-assembly of PEDOT on polydopamine-reduced and sulfonated graphene oxide (PSGD) templates (Fig. 5(c)). The hydrophilic PSGD nanosheets could be easily combined with the hydrogel to prevent aggregation, thereby giving the hydrogel excellent properties, including conductivity, adhesion, and stretchability, which could be used in wearable and implantable bioelectronics applications.

To better combine the conductivity of graphene with the flexibility of hydrogels, unlike traditional graphene composite hydrogels, Cai et al. [182] used the 3D graphene foam obtained by chemical vapor deposition as conductive elements, flexible polyacrylamide/calcium-alginate (PAM/CA) hydrogel as the substrate to obtain a high-performance strain sensor (Fig. 5(d)). Among them, the graphene foam and the hydrogel provided excellent strain responsiveness and skin-like stretchability, respectively. The effective combination of their advantages greatly improved the performance of strain sensors. The strain sensor exhibited an ultra-wide strain range of up to 500% with high gage factor for 1,800 and 1,000 cyclic stability.

5 Application of graphene wearable devices

5.1 Human motion detection (motion, breath, pulse, etc.)

The dynamic movement of different parts of the human body can feedback the key signals needed for clinical diagnosis. Continuous monitoring of human activities through high-sensitivity pressure, tactile, or strain sensors can realize real-time tracking of health conditions, chronic diseases, and movement disorders.

Graphene and its derivatives have made great progress in wearable strain sensors due to their excellent piezoresistive properties and mechanical flexibility. In addition, the cracks of graphene and graphene-like materials also play an important role in improving the piezoresistive effect of wearable sensors. In recent years, graphene-based piezoresistive sensors with different structures and sensing mechanisms have been developed, and their performance in human motion monitoring has also been improved. The performances of each graphene wearable devices are listed in Table 1.

To realize human motion monitoring, wearable sensors need a high sensitivity, fast response, and good durability, which have high requirements for the robustness, ductility, and resilience of the sensor. To manufacture a high-performance strain sensor that can fit the human body, Yang et al. [183] fabricated a wearable graphene textile sensor based on polyester fabrics through a simple thermally reduced GO (Fig. 6(a)). The graphene fabric transverse and longitudinal fiber interweaving structure realized the unique directional sensitivity, high sensitivity, and long-term stability. As shown in Fig. 1, the sensor could be mounted on different joints, such as finger, knee, and wrist, to detect human activities. Graphene textile strain sensors could be woven on clothes to realize real-time and continuous detection of human movement.

In addition, inspired by the force-sensing structure of human skin epidermal tissue, Pang et al. [184] used a simple sandpaper template method to prepare a special surface morphology with randomly distributed spinous processes similar to the epidermis morphology (Fig. 6(b)). The effective interlocking of spinosum microstructure and random distribution achieved a more uniform pressure distribution, and the graphene-based sensor achieves a sensitivity of 25.1 kPa^{-1}. The pressure sensor could be used to monitor the heart rate, breathing state, human activity, voice recognition, etc. In addition, they fixed three graphene sensors on the corresponding insoles for gait detection. The gait detection system showed superior ability to recognize detailed information of walking status, and was expected to be used for the detection of arthritis, neurological diseases, and acquired foot deformities.

Different from the mechanical strain of the large human body movement, the detection of subtle strain and pressure signals on the human body (such as pulse beat, occurrence recognition, and heart rate) has higher requirements for the sensitivity of the sensor. Generally, insufficient sensitivity is mainly due to small external strains that do not induce sufficient variation in the conduction network. Huang et al. [112] proposed a universal and simple method to prepare highly sensitive porous graphene fibers (PGFs) decorated with nanospheres (Fig. 6(c)). This novel structure endowed graphene fibers with ultra-high strain sensing capabilities. PGFs sensors could detect various information, including real-time monitoring of pulse waves, joint movements, and eye movements. PGFs could also be integrated into commercial fabrics for spatial mapping of tactile stimuli.

Heart rate is a direct indicator of our heart health. Continuous and accurate monitoring of heart rate is essential for disease prevention. This also has strict requirements on the sensor, such as high sensitivity to detect small heartbeats, good human body fit to achieve accurate signal capture, and long-term stability to achieve continuous monitoring. Bi et al. [185] prepared an rGO and pen ink/polyvinyl alcohol layered strain sensor based on modal/spandex (MS) fabric through a scalable chemical reduction method (Fig. 6(d)). Compared with the graphene fabric sensor prepared by the traditional CVD method, the conductive MS fabric strain sensor had an ultra-high sensitivity (gauge factor (GF)

Table 1 The performances of graphene wearable devices

Sensing materials	Sensitivity (kPa^{-1})/GF	Detecting range (kPa/%)	Response time/ recovery time (ms)	Detecting limit (Pa/%)	References
Graphene/polyester fabric	GF = −1.7 GF = −26	*x*-axis: 0%–15% *y*-axis: 0%–8%	—	—	[183]
Spinosum microstructure rGO	25.1	0–2.6	120/180	16	[184]
Porous graphene fibers	GF = 51 (strain of 0%–5%) GF = 87 (strain of 5%–8%)	0%–100%	< 100/~ 1,400	0.01%	[112]
rGO/pen ink/polyvinyl fabric	GF = 492.8	0%–300%	—	3%	[185]
rGO pattern/ecoflex	12.3	0–200	—	—	[186]

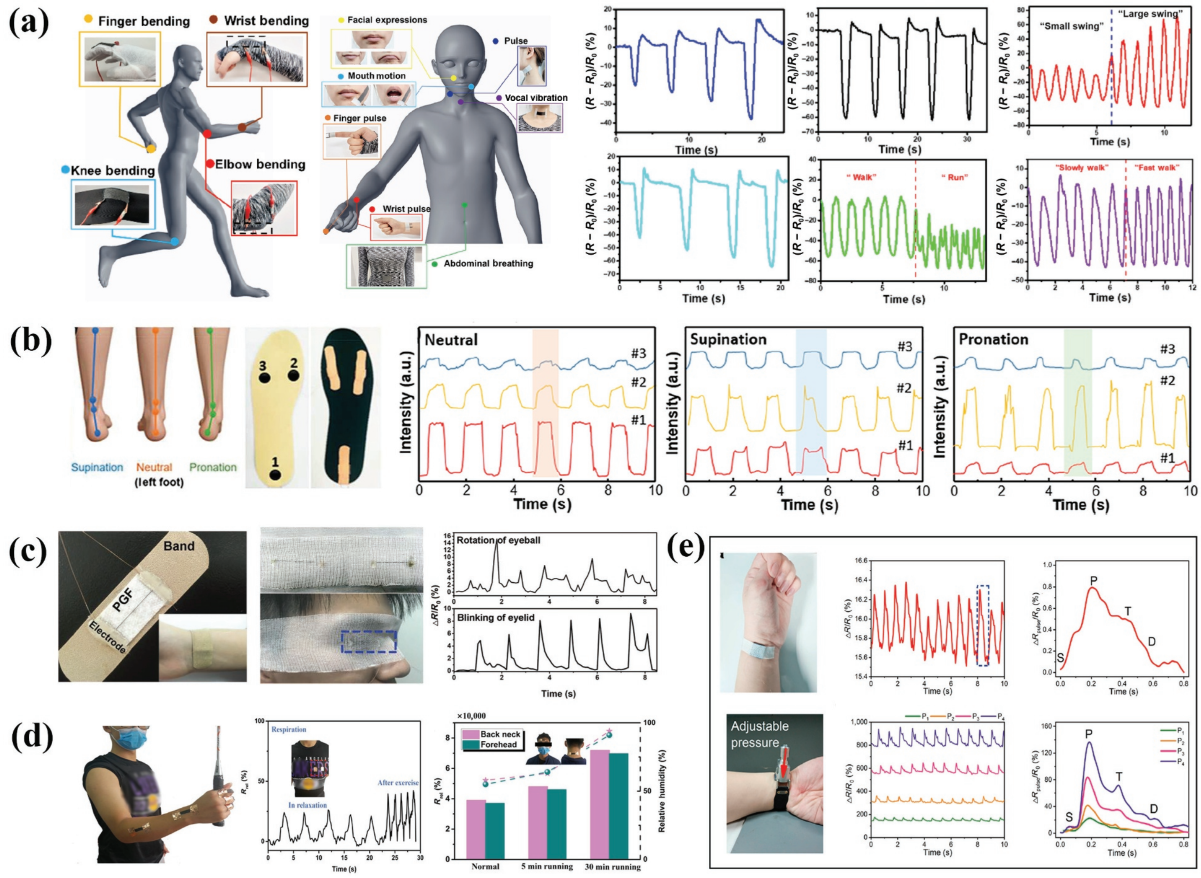

Figure 6 (a) Applications of the wearable graphene textile strain sensors for detecting various human motions. Reproduced with permission from Ref. [183], © American Chemical Society 2018. (b) The photograph of the graphene-based sensor fixed on the insole and its application for gait detection. Reproduced with permission from Ref. [184], © American Chemical Society 2018. (c) The photographs of the homemade monitoring device based on PGFs and its signal detection for eyeball rotation and blinking. Reproduced with permission from Ref. [112], © WILEY-VCH Verlag GmbH & Co. KGaA, Weinheim 2019. (d) Schematic illustration of the human motion monitoring using conductive fabric as a strain sensor. Reproduced with permission from Ref. [185], © American Chemical Society 2020. (e) Schematic illustration of the low-cost flexible pressure sensor attached to the wrist for detecting signals from the arterial pulse. Reproduced with permission from Ref. [186], © American Chemical Society 2020.

of 492.8), wide strain range (~ 300%), good skin conformity, and long-term stability, and could be used for monitoring subtle physiological changes such as heart rate and pulse.

Wu et al. [186] used laser scribing graphene to prepare a flexible pressure sensor with positive resistance–pressure response. (Fig. 6(e)). The sensor could achieve ultra-high sensitivity and wide detection range, average sensitivity can reach 12.3 kPa^{-1}. In addition, the device had a signal amplification characteristic similar to a mechanical triode under an external pressure bias. As shown in Fig. 6(e), based on its amplification ability, the graphene pressure sensor could accurately detect various tiny physiological signals such as pulse detection, showing potential applications in intelligent perception, interactive devices, and real-time health/exercise monitoring.

5.2 Electrophysiological measurement

Exploring a new system and method for convenient and reliable daily health monitoring, non-invasive detection, and early diagnosis of diseases and conditions has always been the pursuit of researchers. However, subtle body signal changes caused by heart or intravascular disease can easily be overwhelmed. Therefore, it is not easy for wearable sensors to realize the non-invasive detection of human health. Active cells or tissues will produce regular electrical phenomena closely related to the state of life at all times. This kind of electrophysiological signal (including resting potentials and action potentials) is essentially the flow of ions across the membrane, which is an important indicator of human health. Therefore, bioelectricity and bioelectrical impedance technology are important means to achieve non-invasive and non-invasive disease detection, prevention, and treatment. ECG, EEG, EMG, and electrooculogram (EOG) are typical bioelectrical signals that are important for disease prevention and treatment. Based on the excellent properties of graphene, graphene composites not only exhibit excellent performance in human motion detection, but also can be used as electrodes to detect typical electrophysiological signals. The performances of graphene electrodes with different structures are listed in Table 2.

5.2.1 ECG

ECG is a technology that records the changes in the electrical activity of the heart caused by the pacemaker, atria, and ventricles in each cardiac cycle through the body surface. According to the different shapes of the electrocardiogram, it can be judged whether the patient has heart disease, such as arrhythmia, myocardial ischemia, and myocardial infarction. Du et al. [187] obtained a new transparent and stretchable graphene electrode by inserting $MoCl_5$ between few-layer graphene (FLG) in a semi-sealed environment (Fig. 7(a)). Based on the nanoconfined doping effect in the sandwich structure, the graphene electrode exhibited high transparency and excellent mechano-electrical stability. When applied as epidermal electrodes, they exhibited excellent ability to detect electrophysiological signals. Compared with the commercial Ag/AgCl electrode, the graphene electrode had a higher signal-to-noise ratio in ECG monitoring. In addition, Pan et al. [188] constructed a proanthocyanins/rGO doped hydrogel with a neural-

Table 2 The performances of graphene electrodes with different structures

Electrode materials	Electrophysiological measurement	Conductivity (Ω/sq, S/m)	Signal-to-noise ratio (dB)	Compliance	References
$MoCl_5$-intercalated bilayer graphene	ECG, EEG, EMG, EOG	40	35.4	200 μm	[187]
Proanthocyanins/rGO/polyvinyl hydrogel	ECG, EMG	—	—	1 mm	[188]
Porous graphene/elastomer sponges	ECG, EEG, EMG,	—	24.1	—	[189]
Graphene/PEDOT:PSS	ECG, EMG, EOG	24	23 ± 0.7	100 nm	[190]
Graphene contact lens electrodes	EOG	1,520	—	Conform to the cornea	[191]
rGO/PEDOT hydrogel	ECG, EEG, EMG	108 S/m	—	Adhesive to human skin	[180]

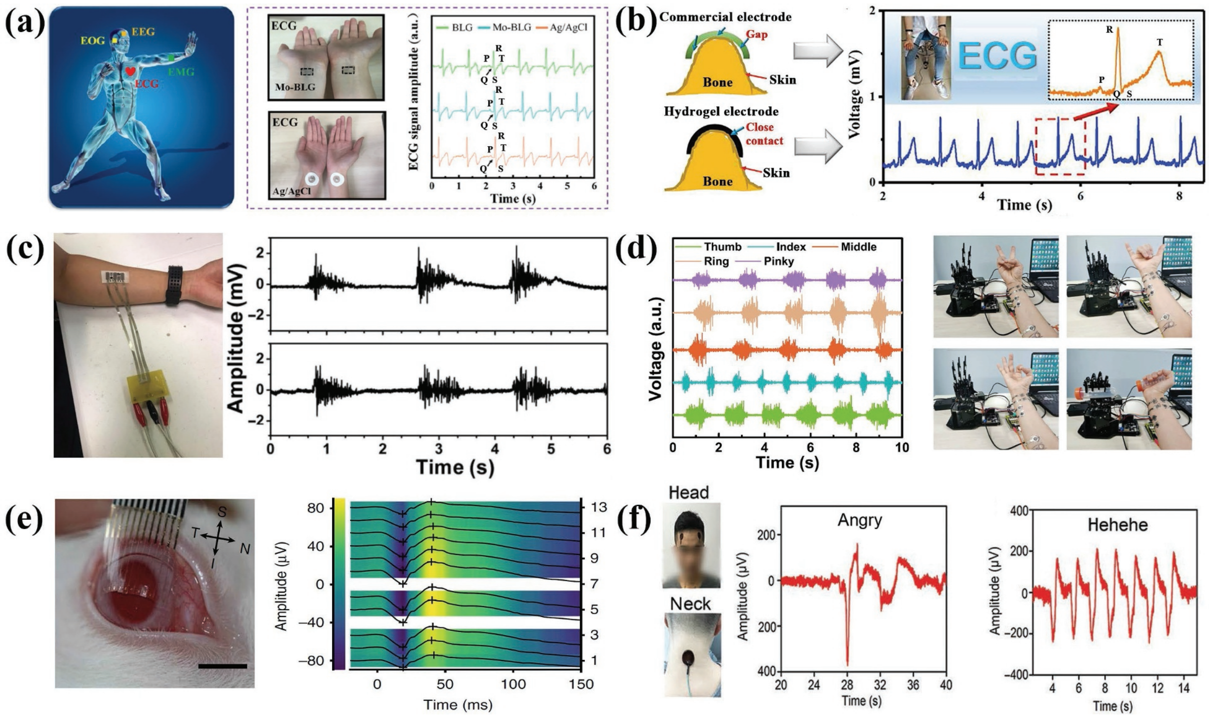

Figure 7 (a) Schematic illustration of the graphene epidermal electrodes intercalating $MoCl_5$ between FLG to detect electrophysiological signals. Reproduced with permission from Ref. [187], © American Chemical Society 2020. (b) The proanthocyanins/rGO doped hydrogel as an electrode used for ECG monitoring. Reproduced with permission from Ref. [188], © Elsevier B.V. 2019. (c) The photograph of the on-skin electronic device based on laser-patterned porous graphene and the display of the EMG signal measured with it. Reproduced with permission from Ref. [189], © WILEY-VCH Verlag GmbH & Co. KGaA, Weinheim 2018. (d) Respiration signals detected by ultra-thin dry epidermal electrodes and applied to control prostheses. Reproduced with permission from Ref. [190], © Zhao, Y. et al. 2021. (e) The GRACE with both flexibility and optical transparency for EOG detection. Reproduced with permission from Ref. [191], © Yin, R. K. et al. 2018. (f) The application of graphene-based biosensors for EEG recording. Reproduced with permission from Ref. [181], © WILEY-VCH Verlag GmbH & Co. KGaA, Weinheim 2019.

like nano-network structure. The modified hydrogel had excellent compliance and adhesion and could be closely attached to human skin. As shown in Fig. 7(b), self-adhesive electrodes assembled from hydrogels could achieve more accurate and stable human ECG signal detection.

5.2.2 EMG

In addition, a new type of electrophysiological signal, EMG, has attracted widespread attention in medical rehabilitation. A weak current is generated when the human muscles contract, and electrodes can be attached to the appropriate position of the skin to measure the current of the muscles on the body's surface. EMG is a method to detect and record the changes in the bioelectric signal of the muscles at rest or around time. It reflects the functional status of neurons, muscles, and peripheral nerves. Sun et al. [189] reported an on-skin electronic device using laser-patterned porous graphene as a sensing component (Fig. 7(c)). The electrode has excellent flexibility and water vapor permeability and could be directly attached to human skin. The graphene electrode exhibited excellent signal transmission performance in EMG measurements under general static and different exercise conditions. In addition, motion artifacts can greatly interfere with the monitoring of EMG signals. Zhao et al. [190] reported an ultra-thin dry epidermal electrode that could closely fit the skin to achieve accurate monitoring of electrophysiological signals. In the signal detection process, it showed low motion artifacts and can realize human–computer interaction and long-term mental/physical health monitoring. As shown in Fig. 7(d), the surface electromyogram (sEMG) signals of different fingers of volunteer could be accurately monitored. In addition, the movement control of the corresponding fingers of the robot hand can be realized by further converting the sEMG signal. This dry and conformal skin electrode could be more complex and accurately applied to control prostheses.

5.2.3 EOG

EOG is a method to objectively and quantitatively detect the function of the retina by recording the slow change of the electrostatic potential of the eye with light adaptation. Currently, EOG signals are used in human activity detection, which can be used to monitor activities such as sleep disorders, reading speed, and eye rotation. Yin et al. [191] reported a graphene contact lens electrode (GRACE) with both flexibility and optical transparency. Compared with the rigid contact lens electrode, the graphene contact lens electrode could form a tight interface with the cornea, showing the advantages of high signal amplitude and stable multifocal electroretinography (mfERG) mapping ability (Fig. 7(e)). This electrode showed the high-efficiency measurement capability of various ERG signals (including full-field electroretinography (ffERG), mfERG, and multi-electrode ERG (meERG)) of cynomolgus monkeys and rabbits.

5.2.4 EEG

In addition, in recent years, EEG is a method of recording brain activity through sophisticated electronic instruments. The electrode records the brain's spontaneous and rhythmic physiological potential changes. It can be used to detect the fields of brain diseases, train attention, control intelligence, etc. Gan et al. [181] reported a graphene-based conductive and adhesive hydrogel that was used to record and collect changes in electrophysiological signals generated by human brain activity. When the tester expressed anger, a sharp EEG peak appeared in the brain waves in Fig. 7(f). When the tester laughed, the hydrogel electrodes could clearly and repeatedly detect brain wave change.

5.3 Multifunctional electronic skin

Natural skin, an organ directly in contact with the outside world, is a multi-functional intelligent sensor that can sense changes in the external environment and feedback to the human body [192, 193]. In recent years, the multi-functional intelligent E-skin with both touch and sensation can imitate, restore, or even replace the human skin, and has been extensively studied in artificial prostheses, soft robots, and embedded sensors [194–198]. With the in-depth research of E-skin, graphene is considered an excellent choice for electronic skin due to its ultrathin, strong toughness, and low resistivity. In addition, both single-layer and multi-layer graphene are suitable for E-skin devices.

How to measure multiple parameters in a single functional device is always a challenge for smart E-skins. Chhetry et al. [199] combined outstanding electrical properties of black phosphorus and laser-engraved graphene (BP@LEG) to construct an E-skin with high-sensitivity, dual-mode temperature, and strain sensing functions (Fig. 8(a)). The dual-parameter temperature–strain E-skin could efficiently and accurately determine that the body temperature and human-body-induced deformations without interfering with each other, fully imitating the perception function of skin to external stimuli.

Qiao et al. [200] proposed a multilayer graphene epidermal skin based on laser scribing graphene and studied the effect of graphene patterns on the performance of electronic skin. As shown in Fig. 8(b), the patterned graphene electronic skin could withstand compression and stretching without causing irreparable damage. When packed into ecoflex and PDMS, the epidermal skin exhibited an ultrahigh gauge factor (up to 673) and long-term stability. The simple process and exquisite patterns give graphene devices great potential in the field of electronic skin. In addition, the generation of micro-cracks in the deformation process of graphene is a key factor affecting sensitivity. Inspired by higher plants, Qiao et al. [201] imitated plasmodesmata and used silver nanowires to bridge laser-scribed graphene oxide. The unique plasmodesmata-like structure greatly improved the performance of mechanical sensitivity and measuring range (Fig. 8(c)).

6 Summary and perspectives

With the rapid development of personalized medicine, the functions and applications of wearable sensors are constantly innovating. The unique structure and physicochemical properties of graphene have triggered researchers' interest as flexible electronic devices in the fields of human–computer interaction and health monitoring. Through proper design of the structure, sensing mechanism, and substrate, wearable sensors based on

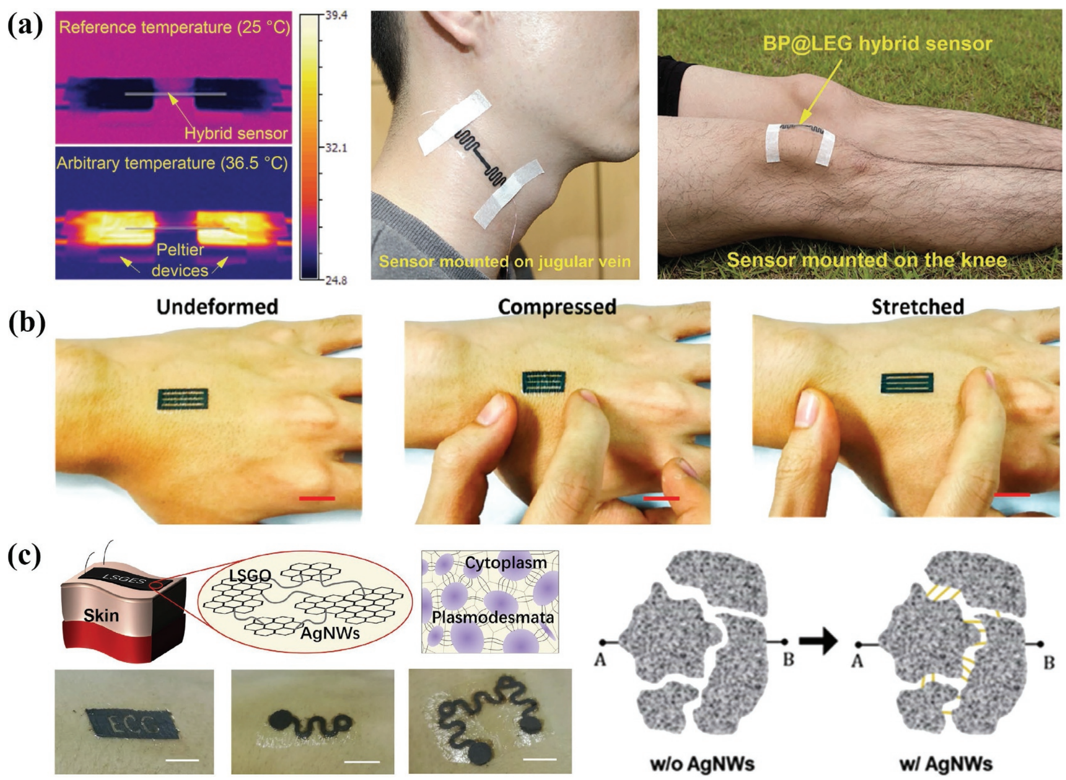

Figure 8 (a) Schematic of BP@LEG E-skin with high-sensitivity dual-mode temperature and strain sensing functions. Reproduced with permission from Ref. [199], © Wiley-VCH GmbH 2020. (b) The demonstration of the patterned graphene electronic skin that can withstand stretching and compression without irreparable destroying. Reproduced with permission from Ref. [200], © American Chemical Society 2018. (c) Schematic illustration of the graphene oxide electronic skin with plasmodesmata-like structure. Reproduced with permission from Ref. [201], © Elsevier Ltd. 2019.

graphene composite materials can have excellent flexibility, sensitivity, response speed, and long-term stability. In this review, we mainly review the latest developments in graphene wearable sensors and briefly discussed some selected cases, including innovative production technology, material design, sensing mechanism, function, and application of graphene sensors. In recent years, graphene sensors have made considerable progress in human motion monitoring, electrophysiological signal monitoring, and multifunctional E-skin.

At present, graphene wearable electronic products are still the subject of in-depth research. For example, graphene sensors still need to be improved in terms of long-term stability and mechanical adaptability to meet different application requirements. The graphene sensor is composed of two parts: a conductive network and a flexible substrate. Graphene itself and the conductive network formed by its irreversibly fracture under repeated external forces, which causes the performance degeneration of the sensor and difficulty to maintain long-term performance stability. In addition, the mechanical constraints of wearable sensors are also an important factor affecting their applications. To keep up with the development of science and technology, it is worth investing a lot of effort to develop some novel functions and apply them in practice, such as the introduction of wireless transmission technology and self-powered technology. We believe that the huge prospects of graphene in the field of wearable electronic devices will have an indispensable impact on human life and health care.

Acknowledgements

This research was supported by a grant from the National Natural Science Foundation of China (NSFC) (No. 51873024) and Science and Technology Research Project of the Education Department of Jilin Province (No. JJKH20210734KJ).

References

[1] Cai, Y. C.; Shen, J.; Dai, Z. Y.; Zang, X. X.; Dong, Q. C.; Guan, G. F.; Li, L. J.; Huang, W.; Dong, X. C. Extraordinarily stretchable all-carbon collaborative nanoarchitectures for epidermal sensors. *Adv. Mater.* **2017**, *29*, 1606411.

[2] Wang, Z. H.; Si, Y.; Zhao, C. Y.; Yu, D.; Wang, W.; Sun, G. Flexible and washable poly(ionic liquid) nanofibrous membrane with moisture proof pressure sensing for real-life wearable electronics. *ACS Appl. Mater. Interfaces* **2019**, *11*, 27200–27209.

[3] Li, M. M.; Chen, X.; Li, X. T.; Dong, J.; Zhao, X.; Zhang, Q. H. Wearable and robust polyimide hydrogel fiber textiles for strain sensors. *ACS Appl. Mater. Interfaces* **2021**, *13*, 43323–43332.

[4] Ding, Y. R.; Xue, C. H.; Guo, X. J.; Wang, X.; Jia, S. T.; An, Q. F. Fabrication of TPE/CNTs film at air/water interface for flexible and superhydrophobic wearable sensors. *Chem. Eng. J.* **2021**, *409*, 128199.

[5] Song, Y.; Min, J. H.; Yu, Y.; Wang, H. B.; Yang, H. X.; Zhang, H. X.; Gao, W. Wireless battery-free wearable sweat sensor powered by human motion. *Sci. Adv.* **2020**, *6*, eaay9842.

[6] Li, Y.; Wang, S.; Xiao, Z. C.; Yang, Y.; Deng, B. W.; Yin, B.; Ke, K.; Yang, M. B. Flexible TPU strain sensors with tunable sensitivity and stretchability by coupling AgNWs with rGO. *J. Mater. Chem. C* **2020**, *8*, 4040–4048.

[7] Lyu, Q.; Gong, S.; Yin, J. L.; Dyson, J. M.; Cheng, W. L. Soft wearable healthcare materials and devices. *Adv. Healthc. Mater.* **2021**, *10*, e2100577.

[8] Qiao, Y. C.; Li, X. S.; Jian, J. M.; Wu, Q.; Wei, Y. H.; Shuai, H.; Hirtz, T.; Zhi, Y.; Deng, G.; Wang, Y. F. et al. Substrate-free multilayer graphene electronic skin for intelligent diagnosis. *ACS Appl. Mater. Interfaces* **2020**, *12*, 49945–49956.

[9] Mandal, S.; Seth, A.; Yadav, V.; Kumari, S.; Kumar, M.; Ojha, U. Nanocomposite grafted stretchable and conductive ionic hydrogels for use as soft electrode in a wearable electrocardiogram monitoring device. *ACS Appl. Polym. Mater.* **2019**, *2*, 618–625.

[10] Yang, J.; Liu, Q.; Deng, Z.; Gong, M.; Lei, F.; Zhang, J.; Zhang, X.; Wang, Q.; Liu, Y.; Wu, Z. et al. Ionic liquid-activated wearable electronics. *Mater. Today Phys.* **2019**, *8*, 78–85.

[11] Zhang, L. J.; Liu, X.; Zhong, M. J.; Zhou, Y. N.; Wang, Y. J.; Yu, T. H.; Xu, X. B.; Shen, W.; Yang, L.; Liu, N. et al. Micro-nano hybrid-structured conductive film with ultrawide range pressure-sensitivity and bioelectrical acquirability for ubiquitous wearable applications. *Appl. Mater. Today* **2020**, *20*, 100651.

[12] Cai, Y. W.; Zhang, X. N.; Wang, G. G.; Li, G. Z.; Zhao, D. Q.; Sun, N.; Li, F.; Zhang, H. Y.; Han, J. C.; Yang, Y. A flexible ultra-sensitive triboelectric tactile sensor of wrinkled PDMS/MXene composite films for E-skin. *Nano Energy* **2021**, *81*, 105663.

[13] Zhou, K. K.; Xu, W.; Yu, Y. F.; Zhai, W.; Yuan, Z. Q.; Dai, K.; Zheng, G. Q.; Mi, L. W.; Pan, C. F.; Liu, C. T. et al. Tunable and nacre-mimetic multifunctional electronic skins for highly stretchable contact-noncontact sensing. *Small* **2021**, *17*, 2100542.

[14] Ameri, S. K.; Ho, R.; Jang, H.; Tao, L.; Wang, Y. H.; Wang, L.; Schnyer, D. M.; Akinwande, D.; Lu, N. S. Graphene electronic tattoo sensors. *ACS Nano* **2017**, *11*, 7634–7641.

[15] Xie, J.; Chen, Q.; Shen, H. J.; Li, G. R. Review—Wearable graphene devices for sensing. *J. Electrochem. Soc.* **2020**, *167*, 037541.

[16] Zhang, K.; Kang, N. W.; Zhang, B.; Xie, R. J.; Zhu, J. Y.; Zou, B. H.; Liu, Y. H.; Chen, Y. Y.; Shi, W.; Zhang, W. N. et al. Skin conformal and antibacterial PPy-leather electrode for ECG monitoring. *Adv. Electron. Mater.* **2020**, *6*, 2000259.

[17] Gao, Y.; Wang, Y. R.; Xia, S.; Gao, G. H. An environment-stable hydrogel with skin-matchable performance for human–machine interface. *Sci. China Mater.* **2021**, *64*, 2313–2324.

[18] Xia, Y. M.; Wu, Y. P.; Yu, T.; Xue, S. S.; Guo, M. L.; Li, J. L.; Li, Z. Y. Multifunctional glycerol-water hydrogel for biomimetic human skin with resistance memory function. *ACS Appl. Mater. Interfaces* **2019**, *11*, 21117–21125.

[19] Yi, F. L.; Guo, F. L.; Li, Y. Q.; Wang, D. Y.; Huang, P.; Fu, S. Y. Polyacrylamide hydrogel composite E-skin fully mimicking human skin. *ACS Appl. Mater. Interfaces* **2021**, *13*, 32084–32093.

[20] Yun, Y.; Nandanapalli, K. R.; Choi, J. H.; Son, W.; Choi, C.; Lee, S. Extremely flexible and mechanically durable planar supercapacitors: High energy density and low-cost power source for E-skin electronics. *Nano Energy* **2020**, *78*, 105356.

[21] Gu, G. Y.; Xu, H. P.; Peng, S.; Li, L.; Chen, S. J.; Lu, T. Q.; Guo, X. J. Integrated soft ionotronic skin with stretchable and transparent hydrogel-elastomer ionic sensors for hand-motion monitoring. *Soft Robot.* **2019**, *6*, 368–376.

[22] Park, H.; Song, C.; Jin, S. W.; Lee, H.; Keum, K.; Lee, Y. H.; Lee, G.; Jeong, Y. R.; Ha, J. S. High performance flexible micro-supercapacitor for powering a vertically integrated skin-attachable strain sensor on a bio-inspired adhesive. *Nano Energy* **2021**, *83*, 105837.

[23] Liu, S. Y.; Meng, X. L.; Zhang, J. W.; Chae, J. A wireless fully-passive acquisition of biopotentials. *Biosens. Bioelectron.* **2019**, *139*, 111336.

[24] Kim, S. J.; Mondal, S.; Min, B. K.; Choi, C. G. Highly sensitive and flexible strain-pressure sensors with cracked paddy-shaped MoS_2/graphene foam/ecoflex hybrid nanostructures. *ACS Appl. Mater. Interfaces* **2018**, *10*, 36377–36384.

[25] Li, Z. K.; Zhang, S. M.; Chen, Y. H.; Ling, H. N.; Zhao, L. B.; Luo, G. X.; Wang, X. C.; Hartel, M. C.; Liu, H.; Xue, Y. M. et al. Gelatin methacryloyl-based tactile sensors for medical wearables. *Adv. Funct. Mater.* **2020**, *30*, 2003601.

[26] Xu, X. W.; Chen, Y. C.; He, P.; Wang, S.; Ling, K.; Liu, L. H.; Lei, P. F.; Huang, X. J.; Zhao, H.; Cao, J. Y. et al. Wearable CNT/$Ti_3C_2T_x$ MXene/PDMS composite strain sensor with enhanced stability for real-time human healthcare monitoring. *Nano Res.* **2021**, *14*, 2875–2883.

[27] Rashkovska, A.; Depolli, M.; Tomašić, I.; Avbelj, V.; Trobec, R. Medical-grade ECG sensor for long-term monitoring. *Sensors (Basel)* **2020**, *20*, 1695.

[28] Cai, P. Q.; Wan, C. J.; Pan, L.; Matsuhisa, N.; He, K.; Cui, Z. Q.; Zhang, W.; Li, C. C.; Wang, J. W.; Yu, J. et al. Locally coupled electromechanical interfaces based on cytoadhesion-inspired hybrids to identify muscular excitation-contraction signatures. *Nat. Commun.* **2020**, *11*, 2183.
[29] Zhang, L.; Kumar, K. S.; He, H.; Cai, C. J.; He, X.; Gao, H. X.; Yue, S. Z.; Li, C. S.; Seet, R. C. S.; Ren, H. L. et al. Fully organic compliant dry electrodes self-adhesive to skin for long-term motion-robust epidermal biopotential monitoring. *Nat. Commun.* **2020**, *11*, 4683.
[30] Peng, B.; Zhao, F. N.; Ping, J. F.; Ying, Y. B. Recent advances in nanomaterial-enabled wearable sensors: Material synthesis, sensor design, and personal health monitoring. *Small* **2020**, *16*, 2002681.
[31] Teymourian, H.; Parrilla, M.; Sempionatto, J. R.; Montiel, N. F.; Barfidokht, A.; Van Echelpoel, R.; De Wael, K.; Wang, J. Wearable electrochemical sensors for the monitoring and screening of drugs. *ACS Sens.* **2020**, *5*, 2679–2700.
[32] Yin, X. Y.; Zhang, Y.; Cai, X. B.; Guo, Q. Q.; Yang, J.; Wang, Z. L. 3D printing of ionic conductors for high-sensitivity wearable sensors. *Mater. Horizons* **2019**, *6*, 767–780.
[33] Li, F. L.; Xu, Z. F.; Hu, H.; Kong, Z. Y.; Chen, C.; Tian, Y.; Zhang, W. W.; Bin Ying, W.; Zhang, R. Y.; Zhu, J. A polyurethane integrating self-healing, anti-aging and controlled degradation for durable and eco-friendly E-skin. *Chem. Eng. J.* **2021**, *410*, 128363.
[34] Abadi, M. B.; Weissing, R.; Wilhelm, M.; Demidov, Y.; Auer, J.; Ghazanfari, S.; Anasori, B.; Mathur, S.; Maleki, H. Nacre-mimetic, mechanically flexible, and electrically conductive silk fibroin-MXene composite foams as piezoresistive pressure sensors. *ACS Appl. Mater. Interfaces* **2021**, *13*, 34996–35007.
[35] Zhang, X. F.; Yang, G. H.; Zong, L.; Jiang, M.; Song, Z. Q.; Ma, C.; Zhang, T. P.; Duan, Y. X.; Zhang, J. M. Tough, ultralight, and water-adhesive graphene/natural rubber latex hybrid aerogel with sandwichlike cell wall and biomimetic rose-petal-like surface. *ACS Appl. Mater. Interfaces* **2020**, *12*, 1378–1386.
[36] Yun, J.; Song, C.; Lee, H.; Park, H.; Jeong, Y. R.; Kim, J. W.; Jin, S. W.; Oh, S. Y.; Sun, L. F.; Zi, G. et al. Stretchable array of high-performance micro-supercapacitors charged with solar cells for wireless powering of an integrated strain sensor. *Nano Energy* **2018**, *49*, 644–654.
[37] Cao, M. H.; Fan, S. Q.; Qiu, H. W.; Su, D. L.; Li, L.; Su, J. CB nanoparticles optimized 3D wearable graphene multifunctional piezoresistive sensor framed by loofah sponge. *ACS Appl. Mater. Interfaces* **2020**, *12*, 36540–36547.
[38] Boland, C. S.; Khan, U.; Binions, M.; Barwich, S.; Boland, J. B.; Weaire, D.; Coleman, J. N. Graphene-coated polymer foams as tuneable impact sensors. *Nanoscale* **2018**, *10*, 5366–5375.
[39] Xu, X.; Guan, C.; Xu, L.; Tan, Y. H.; Zhang, D. W.; Wang, Y. Q.; Zhang, H.; Blackwood, D. J.; Wang, J.; Li, M. et al. Three dimensionally free-formable graphene foam with designed structures for energy and environmental applications. *ACS Nano* **2020**, *14*, 937–947.
[40] Zhou, P. D.; Lin, J.; Zhang, W.; Luo, Z. L.; Chen, L. Z. Photo-thermoelectric generator integrated in graphene-based actuator for self-powered sensing function. *Nano Res.*, in press, https://doi.org10.1007/s12274-021-3791-3.
[41] Chai, Y. Q.; Ma, X. L.; Wang, X. S.; Chen, R. Q.; Jiang, Q. Q.; Zhang, F.; Xie, Z.; Guan, L.; Xue, M. Q. Graphene/high-oriented polypyrrole foam enables new-type ultrasensitive micro-distance detection. *Chem. Eng. J.* **2020**, *402*, 126236.
[42] Hou, C.; Tai, G. A.; Liu, B.; Wu, Z. H.; Yin, Y. H. Borophene–graphene heterostructure: Preparation and ultrasensitive humidity sensing. *Nano Res.* **2020**, *14*, 2337–2344.
[43] Zhang, F.; Feng, Y. Y.; Qin, M. M.; Gao, L.; Li, Z. Y.; Zhao, F. L.; Zhang, Z. X.; Lv, F.; Feng, W. Stress controllability in thermal and electrical conductivity of 3D elastic graphene-crosslinked carbon nanotube sponge/polyimide nanocomposite. *Adv. Funct. Mater.* **2019**, *29*, 1901383.
[44] Zu, G. Q.; Kanamori, K.; Nakanishi, K.; Huang, J. Superhydrophobic ultraflexible triple-network graphene/polyorganosiloxane aerogels for a high-performance multifunctional temperature/strain/pressure sensing array. *Chem. Mater.* **2019**, *31*, 6276–6285.
[45] Yang, L.; Jiang, C.; Yan, J. X.; Shen, Y. F.; Chen, Y.; Xu, L.; Zhu, H. Structuring the reduced graphene oxide/polyHIPE foam for piezoresistive sensing via emulsion-templated polymerization. *Compos. A:Appl. Sci. Manufactur.* **2020**, *134*, 105898.
[46] Xu, H.; Zhang, M. K.; Lu, Y. F.; Li, J. J.; Ge, S. J.; Gu, Z. Z. Dual-mode wearable strain sensor based on graphene/colloidal crystal films for simultaneously detection of subtle and large human motions. *Adv. Mater. Technol.* **2020**, *5*, 1901056.
[47] Li, Z.; Guo, W.; Huang, Y. Y.; Zhu, K. H.; Yi, H. K.; Wu, H. On-skin graphene electrodes for large area electrophysiological monitoring and human–machine interfaces. *Carbon* **2020**, *164*, 164–170.
[48] Cheng, H. N.; Wang, B.; Yang, K.; Yang, Y. Q.; Wang, C. X. A high-performance piezoresistive sensor based on poly(styrene-co-methacrylic acid)@polypyrrole microspheres/graphene-decorated TPU electrospun membrane for human motion detection. *Chem. Eng. J.* **2021**, *426*, 131152.
[49] Zheng, Q. B.; Liu, X.; Xu, H. R.; Cheung, M. S.; Choi, Y. W.; Huang, H. C.; Lei, H. Y.; Shen, X.; Wang, Z. Y.; Wu, Y. et al. Sliced graphene foam films for dual-functional wearable strain sensors and switches. *Nanoscale Horiz.* **2018**, *3*, 35–44.
[50] Manjakkal, L.; Núñez, C. G.; Dang, W. T.; Dahiya, R. Flexible self-charging supercapacitor based on graphene-Ag-3D graphene foam electrodes. *Nano Energy* **2018**, *51*, 604–612.
[51] Wan, S.; Bi, H. C.; Zhou, Y. L.; Xie, X.; Su, S.; Yin, K. B.; Sun, L. T. Graphene oxide as high-performance dielectric materials for capacitive pressure sensors. *Carbon* **2017**, *114*, 209–216.
[52] Ma, Y. X.; Yu, M.; Liu, J. H.; Li, X. J.; Li, S. M. Ultralight interconnected graphene-amorphous carbon hierarchical foam with mechanical resiliency for high sensitivity and durable strain sensors. *ACS Appl. Mater. Interfaces* **2017**, *9*, 27127–27134.
[53] Xia, S.; Song, S. X.; Jia, F.; Gao, G. H. A flexible, adhesive and self-healable hydrogel-based wearable strain sensor for human motion and physiological signal monitoring. *J. Mater. Chem. B* **2019**, *7*, 4638–4648.
[54] Huang, S. C.; Li, J. L.; Zhang, X. Y.; Yang, X. J.; Wang, L. Y.; Li, X. S.; Lü, W. Reduced graphene oxide/polyaniline wrapped carbonized sponge with elasticity for energy storage and pressure sensing. *New J. Chem.* **2021**, *45*, 7860–7866.
[55] Shen, X. P.; Nie, K. C.; Zheng, L.; Wang, Z. S.; Wang, Z.; Li, S.; Jin, C. D.; Sun, Q. F. Muscle-inspired capacitive tactile sensors with superior sensitivity in an ultra-wide stress range. *J. Mater. Chem. C* **2020**, *8*, 5913–5922.
[56] Kim, T.; Park, C.; Samuel, E. P.; An, S.; Aldalbahi, A.; Alotaibi, F.; Yarin, A. L.; Yoon, S. S. Supersonically sprayed washable, wearable, stretchable, hydrophobic, and antibacterial rGO/AgNW fabric for multifunctional sensors and supercapacitors. *ACS Appl. Mater. Interfaces* **2021**, *13*, 10013–10025.
[57] Jia, J.; Huang, G. T.; Deng, J. P.; Pan, K. Skin-inspired flexible and high-sensitivity pressure sensors based on rGO films with continuous-gradient wrinkles. *Nanoscale* **2019**, *11*, 4258–4266.
[58] Ge, G.; Cai, Y. C.; Dong, Q. C.; Zhang, Y. Z.; Shao, J. J.; Huang, W.; Dong, X. C. A flexible pressure sensor based on rGO/polyaniline wrapped sponge with tunable sensitivity for human motion detection. *Nanoscale* **2018**, *10*, 10033–10040.
[59] Ray, T. R.; Choi, J.; Bandodkar, A. J.; Krishnan, S.; Gutruf, P.; Tian, L. M.; Ghaffari, R.; Rogers, J. R. Bio-integrated wearable systems: A comprehensive review. *Chem. Rev.* **2019**, *119*, 5461–5533.
[60] Sun, X.; Yao, F. L.; Li, J. J. Nanocomposite hydrogel-based strain and pressure sensors: A review. *J. Mater. Chem. A* **2020**, *8*, 18605–18623.
[61] Zhu, Y. W.; Murali, S.; Stoller, M. D.; Ganesh, K. J.; Cai, W. W.; Ferreira, P. J.; Pirkle, A.; Wallace, R. M.; Cychosz, K. A.; Thommes, M. et al. Carbon-based supercapacitors produced by activation of graphene. *Science* **2011**, *332*, 1537–1541.
[62] Zhang, H. Q.; He, R. Y.; Niu, Y.; Han, F.; Li, J.; Zhang, X. W.; Xu, F. Graphene-enabled wearable sensors for healthcare monitoring. *Biosens Bioelectron.* **2021**, *197*, 113777.
[63] Yang, Y. B.; Yang, X. D.; Tan, Y. N.; Yuan, Q. Recent progress in flexible and wearable bio-electronics based on nanomaterials. *Nano*

Res. **2017**, *10*, 1560–1583.

[64] Nair, R. R.; Blake, P.; Grigorenko, A. N.; Novoselov, K. S.; Booth, T. J.; Stauber, T.; Peres, N. M. R.; Geim, A. K. Fine structure constant defines visual transparency of graphene. *Science* **2008**, *320*, 1308–1308.

[65] Singh, E.; Meyyappan, M.; Nalwa, H. S. Flexible graphene-based wearable gas and chemical sensors. *ACS Appl. Mater. Interfaces* **2017**, *9*, 34544–34586.

[66] Krishnan, S. K.; Singh, E.; Singh, P.; Meyyappan, M.; Nalwa, H. S. A review on graphene-based nanocomposites for electrochemical and fluorescent biosensors. *RSC Adv.* **2019**, *9*, 8778–8881.

[67] Chang, C.; Chen, W.; Chen, Y.; Chen, Y. H.; Chen, Y.; Ding, F.; Fan, C. H.; Fan, H. J.; Fan, Z. X.; Gong, C. et al. Recent progress on two-dimensional materials. *Acta Phys. Chim. Sin.* **2021**, *37*, 2108017.

[68] Xia, S.; Song, S. X.; Li, Y.; Gao, G. H. Highly sensitive and wearable gel-based sensors with a dynamic physically cross-linked structure for strain-stimulus detection over a wide temperature range. *J. Mater. Chem. C* **2019**, *7*, 11303–11314.

[69] Novoselov, K. S.; Geim, A. K.; Morozov, S. V.; Jiang, D.; Zhang, Y.; Dubonos, S. V.; Grigorieva, I. V.; Firsov, A. A. Electric field effect in atomically thin carbon films. *Science* **2004**, *306*, 666–669.

[70] Qiao, Y. C.; Li, X. S.; Hirtz, T.; Deng, G.; Wei, Y. H.; Li, M. R.; Ji, S. R.; Wu, Q.; Jian, J. M.; Wu, F. et al. Graphene-based wearable sensors. *Nanoscale* **2019**, *11*, 18923–18945.

[71] Cao, Y.; Fatemi, V.; Demir, A.; Fang, S. A.; Tomarken, S. L.; Luo, J. Y.; Sanchez-Yamagishi, J. D.; Watanabe, K.; Taniguchi, T.; Kaxiras, E. et al. Correlated insulator behaviour at half-filling in magic-angle graphene superlattices. *Nature* **2018**, *556*, 80–84.

[72] Ciesielski, A.; Haar, S.; Aliprandi, A.; El Garah, M.; Tregnago, G.; Cotella, G. F.; El Gemayel, M.; Richard, F.; Sun, H. Y.; Cacialli, F. et al. Modifying the size of ultrasound-induced liquid-phase exfoliated graphene: From nanosheets to nanodots. *ACS Nano* **2016**, *10*, 10768–10777.

[73] Silva, A. A.; Pinheiro, R. A.; Rodrigues, A. C.; Baldan, M. R.; Trava-Airoldi, V. J.; Corat, E. J. Graphene sheets produced by carbon nanotubes unzipping and their performance as supercapacitor. *Appl. Surf. Sci.* **2018**, *446*, 201–208.

[74] Kim, K. S.; Zhao, Y.; Jang, H.; Lee, S. Y.; Kim, J. M.; Kim, K. S.; Ahn, J. H.; Kim, P.; Choi, J. Y.; Hong, B. H. Large-scale pattern growth of graphene films for stretchable transparent electrodes. *Nature* **2009**, *457*, 706–710.

[75] Zhao, H. M.; Lin, Y. C.; Yeh, C. H.; Tian, H.; Chen, Y. C.; Xie, D.; Yang, Y.; Suenaga, K.; Ren, T. L.; Chiu, P. W. Growth and Raman spectra of single-crystal trilayer graphene with different stacking orientations. *ACS Nano* **2014**, *8*, 10766–10773.

[76] Xu, X. Z.; Zhang, Z. H.; Dong, J. C.; Yi, D.; Niu, J. J.; Wu, M. H.; Lin, L.; Yin, R. K.; Li, M. Q.; Zhou, J. Y. et al. Ultrafast epitaxial growth of metre-sized single-crystal graphene on industrial Cu foil. *Sci. Bull.* **2017**, *62*, 1074–1080.

[77] Yang, Y.; Fu, Q.; Wei, W.; Bao, X. H. Segregation growth of epitaxial graphene overlayers on Ni(111). *Sci. Bull.* **2016**, *61*, 1536–1542.

[78] Yu, Q.; Jiang, J. C.; Jiang, L. Y.; Yang, Q. Q.; Yan, N. Advances in green synthesis and applications of graphene. *Nano Res.* **2021**, *14*, 3724–3743.

[79] Bae, S.; Kim, H.; Lee, Y.; Xu, X. F.; Park, J. S.; Zheng, Y.; Balakrishnan, J.; Lei, T.; Ri Kim, H.; Song, Y. I. et al. Roll-to-roll production of 30-inch graphene films for transparent electrodes. *Nat. Nanotechnol.* **2010**, *5*, 574–578.

[80] Lee, C.; Wei, X. D.; Kysar, J. W.; Hone, J. Measurement of the elastic properties and intrinsic strength of monolayer graphene. *Science* **2008**, *321*, 385–388.

[81] Balandin, A. A.; Ghosh, S.; Bao, W. Z.; Calizo, I.; Teweldebrhan, D.; Miao, F.; Lau, C. N. Superior thermal conductivity of single-layer graphene. *Nano Lett.* **2008**, *8*, 902–907.

[82] Balandin, A. A. Thermal properties of graphene and nanostructured carbon materials. *Nat. Mater.* **2011**, *10*, 569–581.

[83] Goli, P.; Ning, H.; Li, X. S.; Lu, C. Y.; Novoselov, K. S.; Balandin, A. A. Thermal properties of graphene-copper-graphene heterogeneous films. *Nano Lett.* **2014**, *14*, 1497–1503.

[84] Chen, D. H.; Lin, Z.; Sartin, M. M.; Huang, T. X.; Liu, J.; Zhang, Q. G.; Han, L. H.; Li, J. F.; Tian, Z. Q.; Zhan, D. P. Photosynergetic electrochemical synthesis of graphene oxide. *J. Am. Chem. Soc.* **2020**, *142*, 6516–6520.

[85] Sofer, Z.; Luxa, J.; Jankovský, O.; Sedmidubský, D.; Bystroň, T.; Pumera, M. Synthesis of graphene oxide by oxidation of graphite with ferrate(VI) compounds: Myth or reality? *Angew. Chem., Int. Ed.* **2016**, *55*, 11965–11969.

[86] Wang, Y. F.; Song, C. P.; Yu, X. H.; Liu, L.; Han, Y. C.; Chen, J.; Fu, J. Thermo-responsive hydrogels with tunable transition temperature crosslinked by multifunctional graphene oxide nanosheets. *Compos. Sci. Technol.* **2017**, *151*, 139–146.

[87] Lu, N.; Wang, L. Q.; Lv, M.; Tang, Z. S.; Fan, C. H. Graphene-based nanomaterials in biosystems. *Nano Res.* **2019**, *12*, 247–264.

[88] Kim, S. J.; Song, W.; Yi, Y.; Min, B. K.; Mondal, S.; An, K. S.; Choi, C. G. High durability and waterproofing rGO/SWCNT-fabric-based multifunctional sensors for human-motion detection. *ACS Appl. Mater. Interfaces* **2018**, *10*, 3921–3928.

[89] Yu, T. T.; Zhang, D. G.; Wu, Y. L.; Guo, S. Z.; Lei, F.; Li, Y.; Yang, J. Y. Graphene foam pressure sensor based on fractal electrode with high sensitivity and wide linear range. *Carbon* **2021**, *182*, 497–505.

[90] Zhang, Z. X.; Tang, L.; Chen, C.; Yu, H. T.; Bai, H. H.; Wang, L.; Qin, M. M.; Feng, Y. Y.; Feng, W. Liquid metal-created macroporous composite hydrogels with self-healing ability and multiple sensations as artificial flexible sensors. *J. Mater. Chem. A* **2021**, *9*, 875–883.

[91] Yang, X. L.; Cao, L. Q.; Wang, J. D.; Chen, L. P. Sandwich-like polypyrrole/reduced graphene oxide nanosheets integrated gelatin hydrogel as mechanically and thermally sensitive skinlike bioelectronics. *ACS Sustain. Chem. Eng.* **2020**, *8*, 10726–10739.

[92] Liu, Q.; Zhang, M.; Huang, L.; Li, Y. R.; Chen, J.; Li, C.; Shi, G. Q. High-quality graphene ribbons prepared from graphene oxide hydrogels and their application for strain sensors. *ACS Nano* **2015**, *9*, 12320–12326.

[93] Zhu, Z. C.; Li, Y.; Xu, H.; Peng, X.; Chen, Y. N.; Shang, C.; Zhang, Q.; Liu, J. Q.; Wang, H. L. Tough and thermosensitive poly(N-isopropylacrylamide)/graphene oxide hydrogels with macroscopically oriented liquid crystalline structures. *ACS Appl. Mater. Interfaces* **2016**, *8*, 15637–15644.

[94] Liu, B. T.; Xie, J.; Ma, H.; Zhang, X.; Pan, Y.; Lv, J. W.; Ge, H.; Ren, N.; Su, H. Q.; Xie, X. J. et al. From graphite to graphene oxide and graphene oxide quantum dots. *Small* **2017**, *13*, 1601001.

[95] Lee, S. Y.; Mahajan, R. L. A facile method for coal to graphene oxide and its application to a biosensor. *Carbon* **2021**, *181*, 408–420.

[96] Lee, S. H.; Lee, H. B.; Kim, Y.; Jeong, J. R.; Lee, M. H.; Kang, K. Neurite guidance on laser-scribed reduced graphene oxide. *Nano Lett.* **2018**, *18*, 7421–7427.

[97] Liu, Y. C.; Tu, W. W.; Chen, M. Y.; Ma, L. L.; Yang, B.; Liang, Q. L.; Chen, Y. Y. A mussel-induced method to fabricate reduced graphene oxide/halloysite nanotubes membranes for multifunctional applications in water purification and oil/water separation. *Chem. Eng. J.* **2018**, *336*, 263–277.

[98] Wang, Y. L.; Chen, Y. N.; Lacey, S. D.; Xu, L. S.; Xie, H.; Li, T.; Danner, V. A.; Hu, L. B. Reduced graphene oxide film with record-high conductivity and mobility. *Mater. Today* **2018**, *21*, 186–192.

[99] Gao, X.; Zhang, J.; Ju, P. F.; Liu, J. Z.; Ji, L.; Liu, X. H.; Ma, T. B.; Chen, L.; Li, H. X.; Zhou, H. D. et al. Shear-induced interfacial structural conversion of graphene oxide to graphene at macroscale. *Adv. Funct. Mater.* **2020**, *30*, 2004498.

[100] Feng, H. B.; Cheng, R.; Zhao, X.; Duan, X. F.; Li, J. H. A low-temperature method to produce highly reduced graphene oxide. *Nat. Commun.* **2013**, *4*, 1539.

[101] Jing, X.; Mi, H. Y.; Peng, X. F.; Turng, L. S. Biocompatible, self-healing, highly stretchable polyacrylic acid/reduced graphene oxide nanocomposite hydrogel sensors via mussel-inspired chemistry. *Carbon* **2018**, *136*, 63–72.

[102] Liu, H. B.; Xiang, H. C.; Wang, Y.; Li, Z. J.; Qian, L. W.; Li, P.;

Ma, Y. C.; Zhou, H. W.; Huang, W. A flexible multimodal sensor that detects strain, humidity, temperature, and pressure with carbon black and reduced graphene oxide hierarchical composite on paper. *ACS Appl. Mater. Interfaces* **2019**, *11*, 40613–40619.

[103] Zhu, M.; Yue, Y.; Cheng, Y. F.; Zhang, Y. N.; Su, J.; Long, F.; Jiang, X. L.; Ma, Y. N.; Gao, Y. H. Hollow MXene sphere/reduced graphene aerogel composites for piezoresistive sensor with ultra-high sensitivity. *Adv. Electron. Mater.* **2019**, *6*, 1901064.

[104] Tewari, A.; Gandla, S.; Bohm, S.; McNeill, C. R.; Gupta, D. Highly exfoliated MWNT-rGO ink-wrapped polyurethane foam for piezoresistive pressure sensor applications. *ACS Appl. Mater. Interfaces* **2018**, *10*, 5185–5195.

[105] Wang, Y. L.; Hao, J.; Huang, Z. Q.; Zheng, G. Q.; Dai, K.; Liu, C. T.; Shen, C. Y. Flexible electrically resistive-type strain sensors based on reduced graphene oxide-decorated electrospun polymer fibrous mats for human motion monitoring. *Carbon* **2018**, *126*, 360–371.

[106] Ni, Y. M.; Huang, J. Y.; Li, S. H.; Wang, X. Q.; Liu, L. X.; Wang, M. Y.; Chen, Z.; Li, X.; Lai, Y. K. Underwater, multifunctional superhydrophobic sensor for human motion detection. *ACS Appl. Mater. Interfaces* **2021**, *13*, 4740–4749.

[107] Zou, X. J.; Chai, Y. Q.; Ma, H.; Jiang, Q. Q.; Zhang, W.; Ma, X. L.; Wang, X. S.; Lian, H. Q.; Huang, X. L.; Ji, J. H. et al. Ultrahigh sensitive wearable pressure sensors based on reduced graphene oxide/polypyrrole foam for sign language translation. *Adv. Mater. Technol.* **2021**, *6*, 2001188.

[108] Kang, K.; Park, J.; Kim, K.; Yu, K. J. Recent developments of emerging inorganic, metal and carbon-based nanomaterials for pressure sensors and their healthcare monitoring applications. *Nano Res.* **2021**, *14*, 3096–3111.

[109] Jayathilaka, W. A. D. M.; Qi, K.; Qin, Y. L.; Chinnappan, A.; Serrano-Garcia, W.; Baskar, C.; Wang, H. B.; He, J. X.; Cui, S. Z.; Thomas, S. W. et al. Significance of nanomaterials in wearables: A review on wearable actuators and sensors. *Adv. Mater.* **2019**, *31*, e1805921.

[110] Zeng, Y. Q.; Li, T.; Yao, Y. G.; Li, T. Y.; Hu, L. B.; Marconnet, A. Thermally conductive reduced graphene oxide thin films for extreme temperature sensors. *Adv. Funct. Mater.* **2019**, *29*, 1901388.

[111] Afroj, S.; Tan, S. R.; Abdelkader, A. M.; Novoselov, K. S.; Karim, N. Highly conductive, scalable, and machine washable graphene-based e-textiles for multifunctional wearable electronic applications. *Adv. Funct. Mater.* **2020**, *30*, 2000293.

[112] Huang, T.; He, P.; Wang, R. R.; Yang, S. W.; Sun, J.; Xie, X. M.; Ding, G. Q. Porous fibers composed of polymer nanoball decorated graphene for wearable and highly sensitive strain sensors. *Adv. Funct. Mater.* **2019**, *29*, 1903732.

[113] Sun, S. B.; Liu, Y. Q.; Chang, X. T.; Jiang, Y. C.; Wang, D. S.; Tang, C. J.; He, S. Y.; Wang, M. W.; Guo, L.; Gao, Y. A wearable, waterproof, and highly sensitive strain sensor based on three-dimensional graphene/carbon black/Ni sponge for wirelessly monitoring human motions. *J. Mater. Chem. C* **2020**, *8*, 2074–2085.

[114] Ma, Z. L.; Wei, A. J.; Ma, J. Z.; Shao, L.; Jiang, H. E.; Dong, D. D.; Ji, Z. Y.; Wang, Q.; Kang, S. L. Lightweight, compressible and electrically conductive polyurethane sponges coated with synergistic multiwalled carbon nanotubes and graphene for piezoresistive sensors. *Nanoscale* **2018**, *10*, 7116–7126.

[115] Feng, C. F.; Yi, Z. F.; Jin, X.; Seraji, S. M.; Dong, Y. J.; Kong, L. X.; Salim, N. Solvent crystallization-induced porous polyurethane/graphene composite foams for pressure sensing. *Compos. B:Eng.* **2020**, *194*, 108065.

[116] Cao, X. Y.; Zhang, J.; Chen, S. W.; Varley, R. J.; Pan, K. 1D/2D nanomaterials synergistic, compressible, and response rapidly 3D graphene aerogel for piezoresistive sensor. *Adv. Funct. Mater.* **2020**, *30*, 2003618.

[117] Pang, K.; Song, X.; Xu, Z.; Liu, X. T.; Liu, Y. J.; Zhong, L.; Peng, Y. X.; Wang, J. X.; Zhou, J. Z.; Meng, F. X. et al. Hydroplastic foaming of graphene aerogels and artificially intelligent tactile sensors. *Sci. Adv.* **2020**, *6*, eabd4045.

[118] Xie, Z. H.; Li, H.; Mi, H. Y.; Feng, P. Y.; Liu, Y.; Jing, X. Freezing-tolerant, widely detectable and ultra-sensitive composite organohydrogel for multiple sensing applications. *J. Mater. Chem. C* **2021**, *9*, 10127–10137.

[119] Zheng, C. X.; Lu, K. Y.; Lu, Y.; Zhu, S. L.; Yue, Y. Y.; Xu, X. W.; Mei, C. T.; Xiao, H. N.; Wu, Q. L.; Han, J. Q. A stretchable, self-healing conductive hydrogels based on nanocellulose supported graphene towards wearable monitoring of human motion. *Carbohydr. Polym.* **2020**, *250*, 116905.

[120] Chen, H. J.; Huang, J. R.; Liu, J. T.; Gu, J. F.; Zhu, J. D.; Huang, B.; Bai, J.; Guo, J.; Yang, X.; Guan, L. Q. et al. High toughness multifunctional organic hydrogels for flexible strain and temperature sensor. *J. Mater. Chem. A* **2021**, *9*, 23243–23255.

[121] Xue, B.; Sheng, H.; Li, Y. Q.; Li, L.; Di, W. S.; Xu, Z. Y.; Ma, L. J.; Wang, X.; Jiang, H. T.; Qin, M. et al. Stretchable and self-healable hydrogel artificial skin. *Nat. Sci. Rev.* **2021**, nwab147.

[122] Li, Q. S.; Wu, T. Y.; Zhao, W.; Ji, J. W.; Wang, G. Laser-induced corrugated graphene films for integrated multimodal sensors. *ACS Appl. Mater. Interfaces* **2021**, *13*, 37433–37444.

[123] Ren, H. Y.; Zheng, L. M.; Wang, G. R.; Gao, X.; Tan, Z. J.; Shan, J. Y.; Cui, L. Z.; Li, K.; Jian, M. Q.; Zhu, L. C. et al. Transfer-medium-free nanofiber-reinforced graphene film and applications in wearable transparent pressure sensors. *ACS Nano* **2019**, *13*, 5541–5548.

[124] Moussa, M.; Zhao, Z. H.; El-Kady, M. F.; Liu, H. K.; Michelmore, A.; Kawashima, N.; Majewski, P.; Ma, J. Free-standing composite hydrogel films for superior volumetric capacitance. *J. Mater. Chem. A* **2015**, *3*, 15668–15674.

[125] Xue, P. D.; Chen, C.; Diao, D. F. Ultra-sensitive flexible strain sensor based on graphene nanocrystallite carbon film with wrinkle structures. *Carbon* **2019**, *147*, 227–235.

[126] Wang, M. T.; Qiu, Y. Y.; Jia, J.; Wang, C. Z.; Deng, J. P.; Pan, K. Wavelength-gradient graphene films for pressure-sensitive sensors. *Adv. Mater. Technol.* **2019**, *4*, 1800363.

[127] Ye, X. H.; Qi, M.; Yang, Y. F.; Yu, M.; Huang, T.; Zhang, J. Y.; Yuan, X. B.; Suo, G. Q.; Hou, X. J.; Feng, L. et al. Pattern directive sensing selectivity of graphene for wearable multifunctional sensors via femtosecond laser fabrication. *Adv. Mater. Technol.* **2020**, *5*, 2000446.

[128] Chen, X. P.; Luo, F.; Yuan, M.; Xie, D. L.; Shen, L.; Zheng, K.; Wang, Z. P.; Li, X. D.; Tao, L. Q. A dual-functional graphene-based self-alarm health-monitoring E-Skin. *Adv. Funct. Mater.* **2019**, *29*, 1904706.

[129] Xia, K. L.; Wang, C. Y.; Jian, M. Q.; Wang, Q.; Zhang, Y. Y. CVD growth of fingerprint-like patterned 3D graphene film for an ultrasensitive pressure sensor. *Nano Res.* **2017**, *11*, 1124–1134.

[130] Xu, M. X.; Qi, J. J.; Li, F.; Zhang, Y. Highly stretchable strain sensors with reduced graphene oxide sensing liquids for wearable electronics. *Nanoscale* **2018**, *10*, 5264–5271.

[131] Wang, Y. M.; Wang, Y.; Yang, Y. Graphene-polymer nanocomposite-based redox-induced electricity for flexible self-powered strain sensors. *Adv. Energy Mater.* **2018**, *8*, 1800961.

[132] Dan, L.; Elias, A. L. Flexible and stretchable temperature sensors fabricated using solution-processable conductive polymer composites. *Adv. Healthc. Mater.* **2020**, *9*, 2000380.

[133] Zhang, D. Z.; Xu, Z. Y.; Yang, Z. M.; Song, X. S. High-performance flexible self-powered tin disulfide nanoflowers/reduced graphene oxide nanohybrid-based humidity sensor driven by triboelectric nanogenerator. *Nano Energy* **2020**, *67*, 104251.

[134] Zhang, R. J.; Peng, B.; Yuan, Y. Flexible printed humidity sensor based on poly(3,4-ethylenedioxythiophene)/reduced graphene oxide/Au nanoparticles with high performance. *Compos. Sci. Technol.* **2018**, *168*, 118–125.

[135] Tham, N. C. Y.; Sahoo, P. K.; Kim, Y.; Hegde, C.; Lee, S. W.; Kim, Y. J.; Murukeshan, V. M. Thermally controlled localized porous graphene for integrated graphene-paper electronics. *Adv. Mater. Technol.* **2021**, *6*, 2001156.

[136] Jiang, Y. G.; Liu, M. Y.; Yan, X.; Ono, T.; Feng, L.; Cai, J.; Zhang, D. Y. Electrical breakdown-induced tunable piezoresistivity in graphene/polyimide nanocomposites for flexible force sensor applications. *Adv. Mater. Technol.* **2018**, *3*, 1800113.

[137] Carvalho, A. F.; Fernandes, A. J. S.; Leitão, C.; Deuermeier, J.;

Marques, A. C.; Martins, R.; Fortunato, E.; Costa, F. M. Laser-induced graphene strain sensors produced by ultraviolet irradiation of polyimide. *Adv. Funct. Mater.* **2018**, *28*, 1805271.
[138] Cai, G. M.; Yang, M. Y.; Xu, Z. L.; Liu, J. G.; Tang, B.; Wang, X. G. Flexible and wearable strain sensing fabrics. *Chem. Eng. J.* **2017**, *325*, 396–403.
[139] Karim, N.; Afroj, S.; Tan, S. R.; He, P.; Fernando, A.; Carr, C.; Novoselov, K. S. Scalable production of graphene-based wearable E-textiles. *ACS Nano* **2017**, *11*, 12266–12275.
[140] Afroj, S.; Karim, N.; Wang, Z. H.; Tan, S. R.; He, P.; Holwill, M.; Ghazaryan, D.; Fernando, A.; Novoselov, K. S. Engineering graphene flakes for wearable textile sensors via highly scalable and ultrafast yarn dyeing technique. *ACS Nano* **2019**, *13*, 3847–3857.
[141] Hu, X. R.; Huang, T.; Liu, Z. D.; Wang, G.; Chen, D.; Guo, Q. L.; Yang, S. W.; Jin, Z. W.; Lee, J. M.; Ding, G. Q. Conductive graphene-based E-textile for highly sensitive, breathable, and water-resistant multimodal gesture-distinguishable sensors. *J. Mater. Chem. A* **2020**, *8*, 14778–14787.
[142] Liu, X.; Tang, C.; Du, X. H.; Xiong, S.; Xi, S. Y.; Liu, Y. F.; Shen, X.; Zheng, Q. B.; Wang, Z. Y.; Wu, Y. et al. A highly sensitive graphene woven fabric strain sensor for wearable wireless musical instruments. *Mater. Horiz.* **2017**, *4*, 477–486.
[143] Zheng, Y. J.; Li, Y. L.; Zhou, Y. J.; Dai, K.; Zheng, G. Q.; Zhang, B.; Liu, C. T.; Shen, C. Y. High-performance wearable strain sensor based on graphene/cotton fabric with high durability and low detection limit. *ACS Appl. Mater. Interfaces* **2020**, *12*, 1474–1485.
[144] Zheng, S. D.; Wu, X. T.; Huang, Y. H.; Xu, Z. W.; Yang, W.; Liu, Z. Y.; Yang, M. B. Multifunctional and highly sensitive piezoresistive sensing textile based on a hierarchical architecture. *Compos. Sci. d Technol.* **2020**, *197*, 108255.
[145] Kedambaimoole, V.; Kumar, N.; Shirhatti, V.; Nuthalapati, S.; Nayak, M. M.; Konandur, R. Electric spark induced instantaneous and selective reduction of graphene oxide on textile for wearable electronics. *ACS Appl. Mater. Interfaces* **2020**, *12*, 15527–15537.
[146] Sun, Y. Z.; Zhang, Z. Q.; Zhou, Y.; Liu, S. N.; Xu, H. Wearable strain sensor based on double-layer graphene fabrics for real-time, continuous acquirement of human pulse signal in daily activities. *Adv. Mater. Technol.* **2021**, *6*, 2001071.
[147] Wei, Y. H.; Li, X. S.; Wang, Y. F.; Hirtz, T.; Guo, Z. F.; Qiao, Y. C.; Cui, T. R.; Tian, H.; Yang, Y.; Ren, T. L. Graphene-based multifunctional textile for sensing and actuating. *ACS Nano* **2021**, *15*, 17738–17747.
[148] Han, W. P.; Wu, Y. J.; Gong, H.; Liu, L. X.; Yan, J. X.; Li, M. F.; Long, Y. Z.; Shen, G. Z. Reliable sensors based on graphene textile with negative resistance variation in three dimensions. *Nano Res.* **2021**, *14*, 2810–2818.
[149] Chen, Y. X.; Deng, Z. R.; Ouyang, R.; Zheng, R. H.; Jiang, Z. Q.; Bai, H.; Xue, H. 3D printed stretchable smart fibers and textiles for self-powered e-skin. *Nano Energy* **2021**, *84*, 105866.
[150] Zhao, X.; Xu, L. L.; Chen, Q.; Peng, Q. Y.; Yang, M. L.; Zhao, W. Q.; Lin, Z. S.; Xu, F.; Li, Y. B.; He, X. D. Highly conductive multifunctional rGO/CNT hybrid sponge for electromagnetic wave shielding and strain sensor. *Adv. Mater. Technol.* **2019**, *4*, 1900443.
[151] Braff, M. H.; Di Nardo, A.; Gallo, R. L. Keratinocytes store the antimicrobial peptide cathelicidin in lamellar bodies. *J. Invest. Dermatol.* **2005**, *124*, 394–400.
[152] Zhao, S. F.; Guo, L. Z.; Li, J. H.; Li, N.; Zhang, G. P.; Gao, Y. J.; Li, J.; Cao, D. X.; Wang, W.; Jin, Y. F. et al. Binary synergistic sensitivity strengthening of bioinspired hierarchical architectures based on fragmentized reduced graphene oxide sponge and silver nanoparticles for strain sensors and beyond. *Small* **2017**, *13*, 1700944.
[153] Pei, X. J.; Zhang, H.; Zhou, Y.; Zhou, L. J.; Fu, J. Stretchable, self-healing and tissue-adhesive zwitterionic hydrogels as strain sensors for wireless monitoring of organ motions. *Mater. Horiz.* **2020**, *7*, 1872–1882.
[154] Huang, J. X.; Wang, H. G.; Li, Z. P.; Wu, X. Z.; Wang, J. Q.; Yang, S. R. Improvement of piezoresistive sensing behavior of graphene sponge by polyaniline nanoarrays. *J. Mater. Chem. C* **2019**, *7*, 7386–7394.
[155] Ben-Shimon, Y.; Reddy, S. K.; Ya'akobovitz, A. Graphene foam resonators: Fabrication and characterization. *Nano Res.* **2022**, *15*, 225–229.
[156] Liang, J. J.; Zhao, Z. B.; Tang, Y. C.; Hao, X. J.; Wang, X. Z.; Qiu, J. S. Covalent bonds-integrated graphene foam with superb electromechanical properties as elastic conductor and compressive sensor. *Carbon* **2019**, *147*, 206–213.
[157] Park, H.; Kim, J. W.; Hong, S. Y.; Lee, G.; Kim, D. S.; Oh, J. H.; Jin, S. W.; Jeong, Y. R.; Oh, S. Y.; Yun, J. Y. et al. Microporous polypyrrole-coated graphene foam for high-performance multifunctional sensors and flexible supercapacitors. *Adv. Funct. Mater.* **2018**, *28*, 1707013.
[158] Sengupta, D.; Pei, Y. T.; Kottapalli, A. G. P. Ultralightweight and 3D squeezable graphene-polydimethylsiloxane composite foams as piezoresistive sensors. *ACS Appl. Mater. Interfaces* **2019**, *11*, 35201–35211.
[159] Wang, T. J.; Zhao, J.; Weng, C. X.; Wang, T.; Liu, Y. Y.; Han, Z. P.; Zhang, Z. Three-dimensional graphene coated shape memory polyurethane foam with fast responsive performance. *J. Mater. Chem. C* **2021**, *9*, 7444–7451.
[160] Li, G. C.; Chu, Z. Y.; Gong, X. F.; Xiao, M.; Dong, Q. C.; Zhao, Z. K.; Hu, T. J.; Zhang, Y.; Wang, J.; Tan, Y. L. et al. A wide-range linear and stable piezoresistive sensor based on methylcellulose-reinforced, lamellar, and wrinkled graphene aerogels. *Adv. Mater. Technol.* **2021**, *10*, 2101021.
[161] Ma, Y. N.; Yue, Y.; Zhang, H.; Cheng, F.; Zhao, W. Q.; Rao, J. Y.; Luo, S. J.; Wang, J.; Jiang, X. L.; Liu, Z. T. et al. 3D synergistical MXene/reduced graphene oxide aerogel for a piezoresistive sensor. *ACS Nano* **2018**, *12*, 3209–3216.
[162] Xiao, J. L.; Tan, Y. Q.; Song, Y. H.; Zheng, Q. A flyweight and superelastic graphene aerogel as a high-capacity adsorbent and highly sensitive pressure sensor. *J. Mater. Chem. A* **2018**, *6*, 9074–9080.
[163] Yang, C. X.; Liu, W. J.; Liu, N. S.; Su, J.; Li, L. Y.; Xiong, L.; Long, F.; Zou, Z. G.; Gao, Y. H. Graphene aerogel broken to fragments for a piezoresistive pressure sensor with a higher sensitivity. *ACS Appl. Mater. Interfaces* **2019**, *11*, 33165–33172.
[164] Huang, H. Z.; Su, S.; Wu, N.; Wan, H.; Wan, S.; Bi, H. C.; Sun, L. T. Graphene-based sensors for human health monitoring. *Front. Chem.* **2019**, *7*, 399.
[165] Long, S. S.; Feng, Y. C.; He, F. L.; He, S. S.; Hong, H. C.; Yang, X. R.; Zheng, L. L.; Liu, J.; Gan, L. H.; Long, M. N. An ultralight, supercompressible, superhydrophobic and multifunctional carbon aerogel with a specially designed structure. *Carbon* **2020**, *158*, 137–145.
[166] Huang, J. K.; Zeng, J. B.; Liang, B. Q.; Wu, J. W.; Li, T. G.; Li, Q.; Feng, F.; Feng, Q. W.; Rood, M. J.; Yan, Z. F. Multi-arch-structured all-carbon aerogels with superelasticity and high fatigue resistance as wearable sensors. *ACS Appl. Mater. Interfaces* **2020**, *12*, 16822–16830.
[167] Lü, X. Z.; Yu, T. T.; Meng, F. C.; Bao, W. M. Wide-range and high-stability flexible conductive graphene/thermoplastic polyurethane foam for piezoresistive sensor applications. *Adv. Mater. Technol.* **2021**, *6*, 2100248.
[168] Guan, H.; Dai, X. J.; Ni, L.; Hu, J. H.; Wang, X. Q. Highly elastic and fatigue-resistant graphene-wrapped lamellar wood sponges for high-performance piezoresistive sensors. *ACS Sustain. Chem. Eng.* **2021**, *9*, 15267–15277.
[169] Ying, B. B.; Wu, Q. Y.; Li, J. Y.; Liu, X. Y. An ambient-stable and stretchable ionic skin with multimodal sensation. *Mater. Horiz.* **2020**, *7*, 477–488.
[170] Sun, J. Y.; Keplinger, C.; Whitesides, G. M.; Suo, Z. G. Ionic skin. *Adv. Mater.* **2014**, *26*, 7608–7614.
[171] Lei, Z. Y.; Zhu, W. C.; Zhang, X. C.; Wang, X. J.; Wu, P. Y. Bio-inspired ionic skin for theranostics. *Adv. Funct. Mater.* **2020**, *31*, 2008020.
[172] Xia, S.; Zhang, Q.; Song, S. X.; Duan, L. J.; Gao, G. H. Bioinspired dynamic cross-linking hydrogel sensors with skin-like strain and pressure sensing behaviors. *Chem. Mater.* **2019**, *31*, 9522–9531.
[173] Xia, S.; Song, S. X.; Gao, G. H. Robust and flexible strain sensors based on dual physically cross-linked double network hydrogels for monitoring human-motion. *Chem. Eng. J.* **2018**, *354*, 817–824.

[174] Zhang, Z. Y.; Zheng, Z.; Zhao, Y. L.; Hu, J. H.; Wang, H. T. Highly stretchable porous composite hydrogels with stable conductivity for strain sensing. *Compos. Sci. Technol.* **2021**, *213*, 108968.
[175] Fan, L.; Xie, J. L.; Zheng, Y. P.; Wei, D. X.; Yao, D. D.; Zhang, J.; Zhang, T. D. Antibacterial, self-adhesive, recyclable, and tough conductive composite hydrogels for ultrasensitive strain sensing. *ACS Appl. Mater. Interfaces* **2020**, *12*, 22225–22236.
[176] Wu, J.; Huang, W. X.; Liang, Y. N.; Wu, Z. X.; Zhong, B. Z.; Zhou, Z. J.; Ye, J. D.; Tao, K.; Zhou, Y. B.; Xie, X. Self-calibrated, sensitive, and flexible temperature sensor based on 3D chemically modified graphene hydrogel. *Adv. Electron. Mater.* **2021**, *7*, 2001084.
[177] Zhan, Y. H.; Hao, S.; Li, Y. C.; Santillo, C.; Zhang, C. M.; Sorrentino, L.; Lavorgna, M.; Xia, H. S.; Chen, Z. M. High sensitivity of multi-sensing materials based on reduced graphene oxide and natural rubber: The synergy between filler segregation and macro-porous morphology. *Compos. Sci. Technol.* **2021**, *205*, 108689.
[178] Yang, H. S.; Li, Z. L.; Sun, G. Q.; Jin, X. T.; Lu, B.; Zhang, P. P.; Lin, T. Y.; Qu, L. T. Superplastic air-dryable graphene hydrogels for wet-press assembly of ultrastrong superelastic aerogels with infinite macroscale. *Adv. Funct. Mater.* **2019**, *29*, 1901917.
[179] He, F. L.; You, X. Y.; Gong, H.; Yang, Y.; Bai, T.; Wang, W. G.; Guo, W. X.; Liu, X. Y.; Ye, M. D. Stretchable, biocompatible, and multifunctional silk fibroin-based hydrogels toward wearable strain/pressure sensors and triboelectric nanogenerators. *ACS Appl. Mater. Interfaces* **2020**, *12*, 6442–6450.
[180] Han, L.; Lu, X.; Wang, M. H.; Gan, D. L.; Deng, W. L.; Wang, K. F.; Fang, L. M.; Liu, K. Z.; Chan, C. W.; Tang, Y. H. et al. A mussel-inspired conductive, self-adhesive, and self-healable tough hydrogel as cell stimulators and implantable bioelectronics. *Small* **2017**, *13*, 1601916.
[181] Gan, D. L.; Huang, Z. Q.; Wang, X.; Jiang, L. L.; Wang, C. M.; Zhu, M. Y.; Ren, F. Z.; Fang, L. M.; Wang, K. F.; Xie, C. M. et al. Graphene oxide-templated conductive and redox-active nanosheets incorporated hydrogels for adhesive bioelectronics. *Adv. Funct. Mater.* **2019**, *30*, 1907678.
[182] Cai, Y. T.; Qin, J. B.; Li, W. M.; Tyagi, A.; Liu, Z. J.; Hossain, M. D.; Chen, H. M.; Kim, J. K.; Liu, H. W.; Zhuang, M. H. et al. A stretchable, conformable, and biocompatible graphene strain sensor based on a structured hydrogel for clinical application. *J. Mater. Chem. A* **2019**, *7*, 27099–27109.
[183] Yang, Z.; Pang, Y.; Han, X. L.; Yang, Y. F.; Ling, J.; Jian, M. Q.; Zhang, Y. Y.; Yang, Y.; Ren, T. L. Graphene textile strain sensor with negative resistance variation for human motion detection. *ACS Nano* **2018**, *12*, 9134–9141.
[184] Pang, Y.; Zhang, K. N.; Yang, Z.; Jiang, S.; Ju, Z. Y.; Li, Y. X.; Wang, X. F.; Wang, D. Y.; Jian, M. Q.; Zhang, Y. Y. et al. Epidermis microstructure inspired graphene pressure sensor with random distributed spinosum for high sensitivity and large linearity. *ACS Nano* **2018**, *12*, 2346–2354.
[185] Bi, S. Y.; Hou, L.; Dong, W. W.; Lu, Y. X. Multifunctional and ultrasensitive-reduced graphene oxide and pen ink/polyvinyl alcohol-decorated modal/spandex fabric for high-performance wearable sensors. *ACS Appl. Mater. Interfaces* **2021**, *13*, 2100–2109.
[186] Wu, Q.; Qiao, Y. C.; Guo, R.; Naveed, S.; Hirtz, T.; Li, X. S.; Fu, Y. X.; Wei, Y. H.; Deng, G.; Yang, Y. et al. Triode-mimicking graphene pressure sensor with positive resistance variation for physiology and motion monitoring. *ACS Nano* **2020**, *14*, 10104–10114.
[187] Du, X. J.; Jiang, W. C.; Zhang, Y.; Qiu, J. K.; Zhao, Y.; Tan, Q. S.; Qi, S. Y.; Ye, G.; Zhang, W. F.; Liu, N. Transparent and stretchable graphene electrode by intercalation doping for epidermal electrophysiology. *ACS Appl. Mater. Interfaces* **2020**, *12*, 56361–56371.
[188] Pan, X. F.; Wang, Q. H.; He, P.; Liu, K.; Ni, Y. H.; Chen, L. H.; Ouyang, X. H.; Huang, L. L.; Wang, H. P.; Xu, S. Y. A bionic tactile plastic hydrogel-based electronic skin constructed by a nerve-like nanonetwork combining stretchable, compliant, and self-healing properties. *Chem. Eng. J.* **2020**, *379*, 122271.
[189] Sun, B. H.; McCay, R. N.; Goswami, S.; Xu, Y. D.; Zhang, C.; Ling, Y.; Lin, J.; Yan, Z. Gas-permeable, multifunctional on-skin electronics based on laser-induced porous graphene and sugar-templated elastomer sponges. *Adv. Mater.* **2018**, *30*, e1804327.
[190] Zhao, Y.; Zhang, S.; Yu, T. H.; Zhang, Y.; Ye, G.; Cui, H.; He, C. Z.; Jiang, W. C.; Zhai, Y.; Lu, C. M. et al. Ultra-conformal skin electrodes with synergistically enhanced conductivity for long-time and low-motion artifact epidermal electrophysiology. *Nat. Commun.* **2021**, *12*, 4880.
[191] Yin, R. K.; Xu, Z.; Mei, M.; Chen, Z. L.; Wang, K.; Liu, Y. L.; Tang, T.; Priydarshi, M. K.; Meng, X. J.; Zhao, S. Y. et al. Soft transparent graphene contact lens electrodes for conformal full-cornea recording of electroretinogram. *Nat. Commun.* **2018**, *9*, 2334.
[192] Yue, Z. Y.; Wang, Y.; Lin, Y.; Jia, C. Y. Fully integrated pressure-controlled electrochromic E-skins. *J. Mater. Chem. A* **2021**, *9*, 9134–9144.
[193] Zhang, X. H.; Sheng, N. N.; Wang, L. N.; Tan, Y. Q.; Liu, C. Z.; Xia, Y. Z.; Nie, Z. H.; Sui, K. Y. Supramolecular nanofibrillar hydrogels as highly stretchable, elastic and sensitive ionic sensors. *Mater. Horiz.* **2019**, *6*, 326–333.
[194] Miao, P.; Wang, J.; Zhang, C. C.; Sun, M. Y.; Cheng, S. S.; Liu, H. Graphene nanostructure-based tactile sensors for electronic skin applications. *Nano-Micro Lett.* **2019**, *11*, 71.
[195] Xiang, S. X.; Liu, D. J.; Jiang, C. C.; Zhou, W. M.; Ling, D.; Zheng, W. T.; Sun, X. P.; Li, X.; Mao, Y. C.; Shan, C. X. Liquid-metal-based dynamic thermoregulating and self-powered electronic skin. *Adv. Funct. Mater.* **2021**, *31*, 2100940.
[196] Zhang, Y. J.; Zhao, Y.; Zhai, W.; Zheng, G. Q.; Ji, Y. X.; Dai, K.; Mi, L. W.; Zhang, D. B.; Liu, C. T.; Shen, C. Y. Multifunctional interlocked e-skin based on elastic micropattern array facilely prepared by hot-air-gun. *Chem. Eng. J.* **2021**, *407*, 127960.
[197] Bu, Y. B.; Shen, T. Y.; Yang, W. K.; Yang, S. Y.; Zhao, Y.; Liu, H.; Zheng, Y. J.; Liu, C. T.; Shen, C. Y. Ultrasensitive strain sensor based on superhydrophobic microcracked conductive $Ti_3C_2T_x$ MXene/paper for human-motion monitoring and E-skin. *Sci. Bull.* **2021**, *66*, 1849–1857.
[198] Kim, M. H.; Cho, C. H.; Kim, J. S.; Nam, T. U.; Kim, W. S.; Il Lee, T.; Oh, J. Y. Thermoelectric energy harvesting electronic skin (e-skin) patch with reconfigurable carbon nanotube clays. *Nano Energy* **2021**, *87*, 106156.
[199] Chhetry, A.; Sharma, S.; Barman, S. C.; Yoon, H.; Ko, S.; Park, C.; Yoon, S.; Kim, H.; Park, J. Y. Black phosphorus@laser-engraved graphene heterostructure-based temperature–strain hybridized sensor for electronic-skin applications. *Adv. Funct. Mater.* **2020**, *31*, 2007661.
[200] Qiao, Y. C.; Wang, Y. F.; Tian, H.; Li, M. R.; Jian, J. M.; Wei, Y. H.; Tian, Y.; Wang, D. Y.; Pang, Y.; Geng, X. S. et al. Multilayer graphene epidermal electronic skin. *ACS Nano* **2018**, *12*, 8839–8846.
[201] Qiao, Y. C.; Wang, Y. F.; Jian, J. M.; Li, M. R.; Jiang, G. Y.; Li, X. S.; Deng, G.; Ji, S. R.; Wei, Y. H.; Pang, Y. et al. Multifunctional and high-performance electronic skin based on silver nanowires bridging graphene. *Carbon* **2020**, *156*, 253–260.